Stockwork
GeoConsulting Ltd.

UNIVERSITATEA BABEȘ-BOLYAI
BABEȘ-BOLYAI TUDOMÁNYEGYETEM
BABEȘ-BOLYAI UNIVERSITÄT
BABEȘ-BOLYAI UNIVERSITY
TRADITIO ET EXCELLENTIA

Review of new and innovative analytical methodologies in exploration geochemistry

István MÁRTON, PhD

Lecture D2U1 – part I.

DIM ESEE 2: IMPLEMENTING INNOVATIONS

Innovation in Exploration

Dubrovnik, Croatia / hybrid mode -
October 20th – 22nd, 2021

About the lecturer

Name: István MÁRTON
Title: PhD
Institution: Stockwork Geoconsulting Ltd & Babeş–Bolyai University (Cluj, Romania)
Relevant website: https://scholar.google.com/citations?user=NRvSb2EAAAAJ&hl=en

Email: Istvan.Marton@stockwork.ro

István Márton has obtained BSc and Msc in Romania at the Babeș–Bolyai University, Cluj and University of Bucharest, respectively. Following a 3 years period working as Exploration Geologist in Apuseni Mts (Romania) he continued studies at the University of Geneva (Switzerland), where he obtained PhD in 2008. After a short academic post-doc research period he has joined the exploration industry and since then, he has been working in the exploration and mining industry as an Exploration Geologist and Geochemist.

The lecturer has been involved in target generation, greenfield- and brownfield- exploration and geometallurgical works in 8 countries being focused on Cretaceous–Miocene epithermal Au-Ag, polymetallic carbonate replacement Pb-Zn-Cu-Au, porphyry Cu-Au-Mo, sedimentary rock-hosted gold and Archean orogenic gold deposits. Since 2009 he is working also as visiting lecturer at the University of Babeş–Bolyai University teaching Introduction to Ore Deposits and Economic Geology courses and supervises bachelor/master student projects. More recently the Lecturer is acting as principal geoscientist consultant at Dundee Precious Metals with focus on exploration geochemistry, 3D modelling and drill target generation efforts of the company in greenfield and near-mine projects in Bulgaria, Serbia, Armenia and Canada.

Content

Recent developments in exploration geochemistry and better instrumentation of industrial geochemical laboratories provide large and high-precision partial digestion multi-element datasets for mineral exploration projects. Additionally, the expansion of portable and benchtop XRF, SWIR and XRD devices deliver fast and reliable characterization of mineralogy and geochemistry of drill core, soil and rock samples. Furthermore, tripod- and UAV-based hyperspectral scanning and satellite-based remote sensing deliver high-resolution alteration and lithology maps for pits, underground galleries and surface outcrops. These exploration geochemical datasets provide critical information about ore genetic and mineralization controlling aspects, about alteration footprint and optimal drill-spacing, about vectors to fertile host rocks and economic mineralization and on perspectives of geometallurgical domaining at any mineral exploration project.
The first part of the lesson will provide insights on the use of these exploration geochemical tools and interpretations:

1. Advancements in laboratory analytical methodologies for whole rock analysis (exploration geochemistry)

2. Application of portable or benchtop field XRF instruments

3. VNIR-SWIR spectroscopy (portable and core scan)

4. Hypercloud Spectral Mapping of Pit Walls and Outcrops

5. Satellite-based remote sensing in mineral exploration

6. Distal $^{13}C/^{12}C$ and $^{18}O/^{16}O$ isotopes footprints in carbonate-hosted ore deposits

Advancements in laboratory analytical methodologies for whole rock analysis (exploration geochemistry)

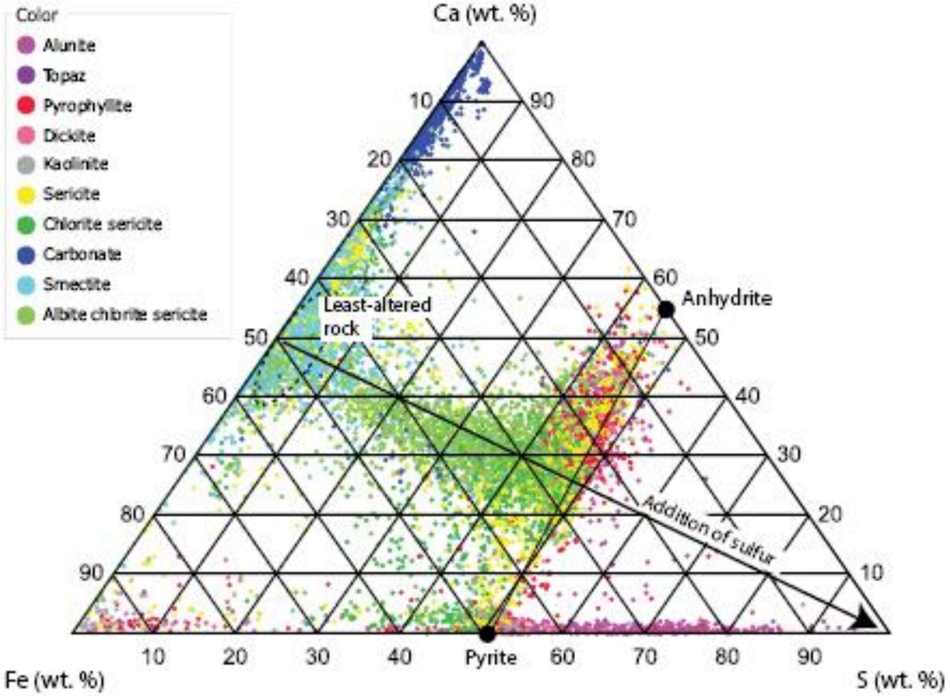

Analytical methodologies in exploration geochemistry

Role of partial digest methods in exploration geochemistry

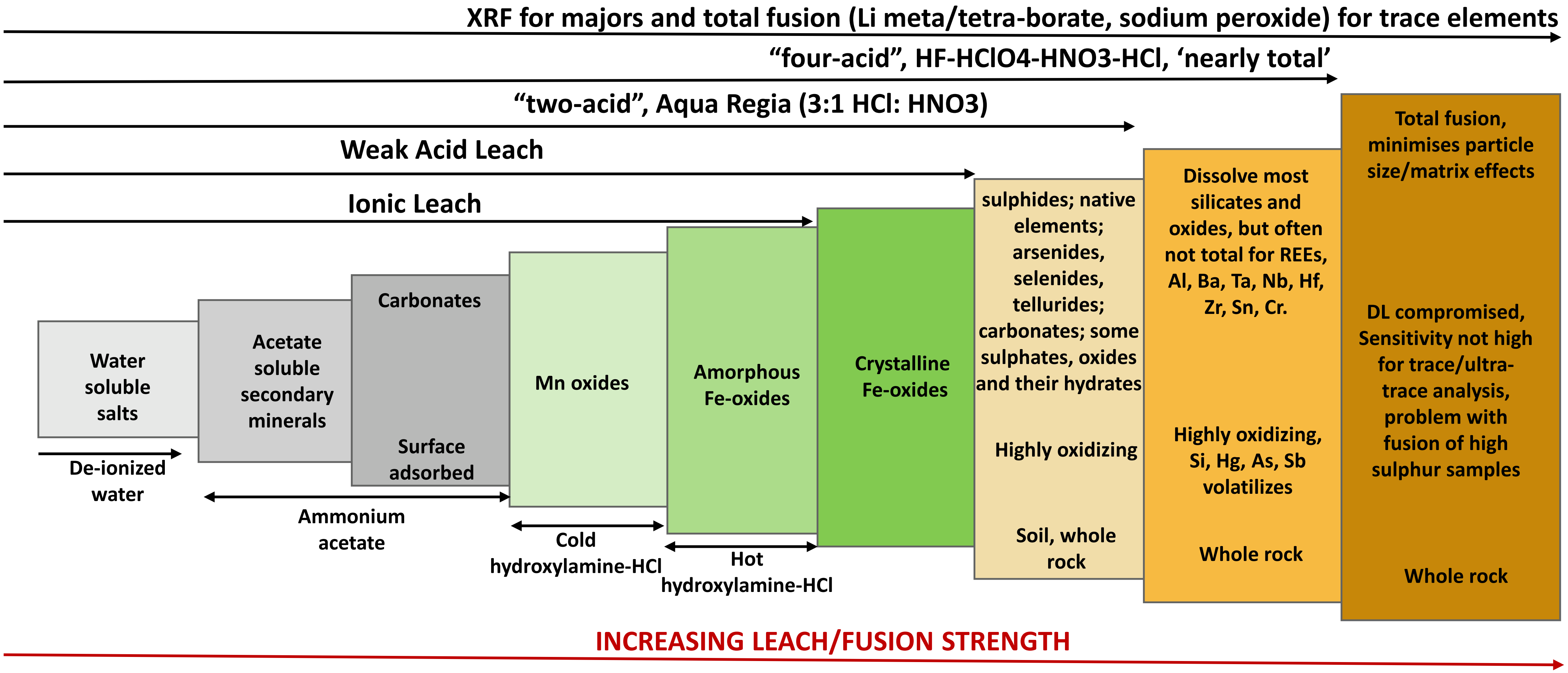

XRF for majors and total fusion (Li meta/tetra-borate, sodium peroxide) for trace elements

“four-acid”, HF-HClO4-HNO3-HCl, ‘nearly total’

“two-acid”, Aqua Regia (3:1 HCl: HNO3)

Weak Acid Leach

Ionic Leach

Water soluble salts

De-ionized water

Acetate soluble secondary minerals

Carbonates

Surface adsorbed

Ammonium acetate

Mn oxides

Cold hydroxylamine-HCl

Amorphous Fe-oxides

Hot hydroxylamine-HCl

Crystalline Fe-oxides

sulphides; native elements; arsenides, selenides, tellurides; carbonates; some sulphates, oxides and their hydrates

Highly oxidizing

Soil, whole rock

Dissolve most silicates and oxides, but often not total for REEs, Al, Ba, Ta, Nb, Hf, Zr, Sn, Cr.

Highly oxidizing, Si, Hg, As, Sb volatilizes

Whole rock

Total fusion, minimises particle size/matrix effects

DL compromised, Sensitivity not high for trace/ultra-trace analysis, problem with fusion of high sulphur samples

Whole rock

INCREASING LEACH/FUSION STRENGTH

- Other element-specific methods (e.g., F by fusion and ISE, C and S by LEKO furnace, Hg by cold-vapor AAS, etc)
- **ICP-MS and ICP-ES** finish provides ppb level detection limits, **AAS finish** provides ppm level detection

Analytical methodologies in exploration geochemistry

Choosing the analytical method

- ICP-MS and ICP-ES finish provides ppb level detection limits, AAS finish provides ppm level detection limits for 2-acid and 4-acid digestion methodologies
- Total or partial elemental composition
- Elements and detection limits required
- Matrix suitable for method
- Use of orientation survey!
- Accuracy and precision required: ‘fit for purpose’
- Representative size of sample or size limitation
- **Cost**

✓ ***Does not exist “best method”!***

✓ ***Always consider/state the sample preparation, digestion AND the analytical technique: these describes the methodology!***

Analytical methodologies in exploration geochemistry

Choosing the analytical method: 2 acid ICP-AES vs 4 acid ICP-MS methods

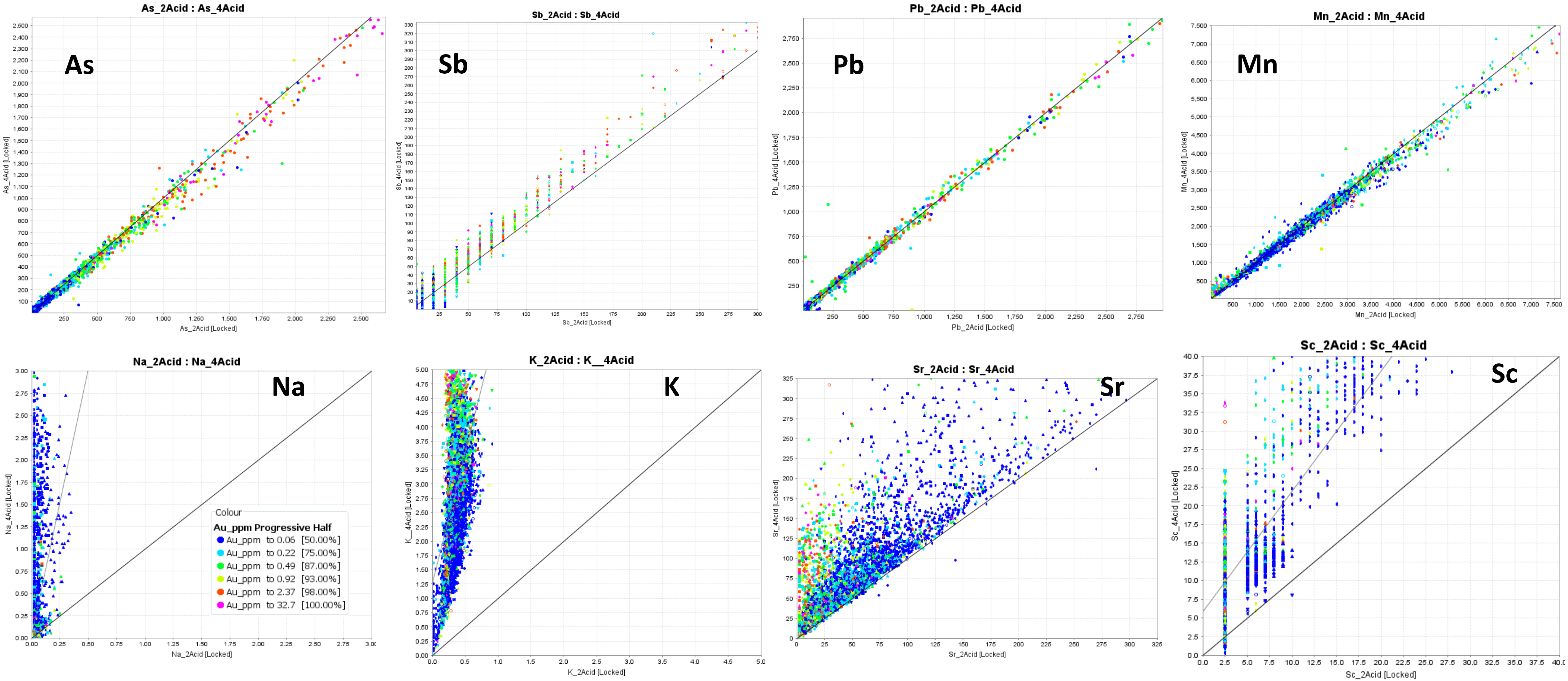

- Drill core samples (whole rock) from epithermal deposit (Romania)

Analytical methodologies in exploration geochemistry

Choosing the analytical method: total fusion vs. 4 acid ICP-MS

Colour

Alteration Box Plot:

- 🟥 AAA_highSr
- 🟨 Phyllic
- 🟩 Unaltered Box
- 🟦 Weak Sericite

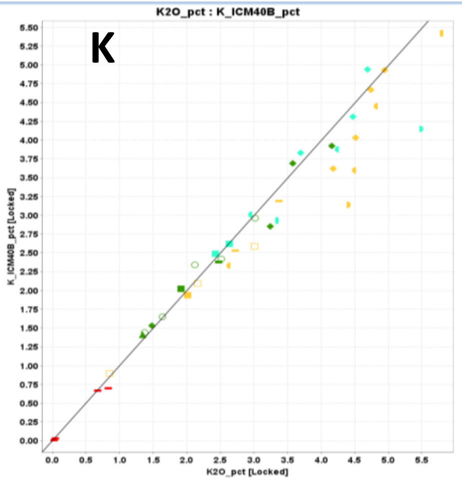
K2O_pct : K_ICM40B_pct

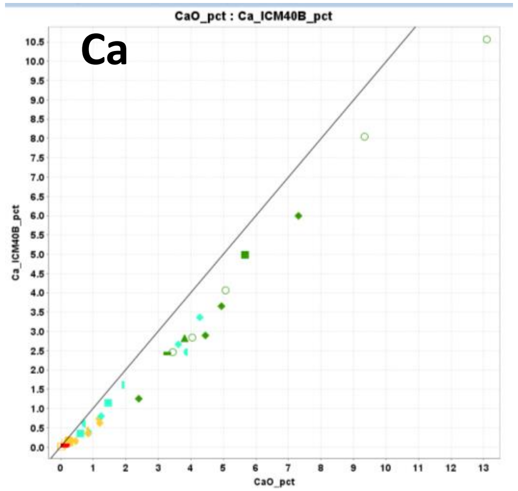
CaO_pct : Ca_ICM40B_pct

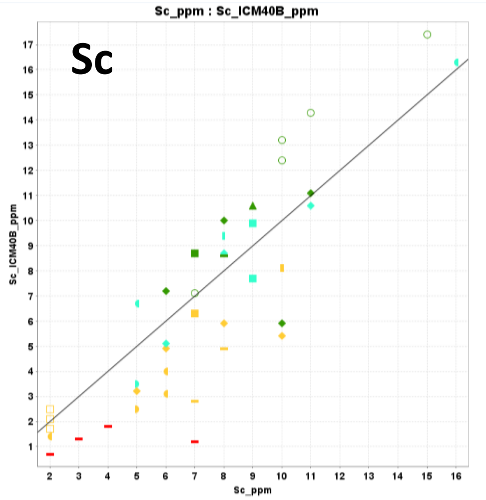
Sc_ppm : Sc_ICM40B_ppm

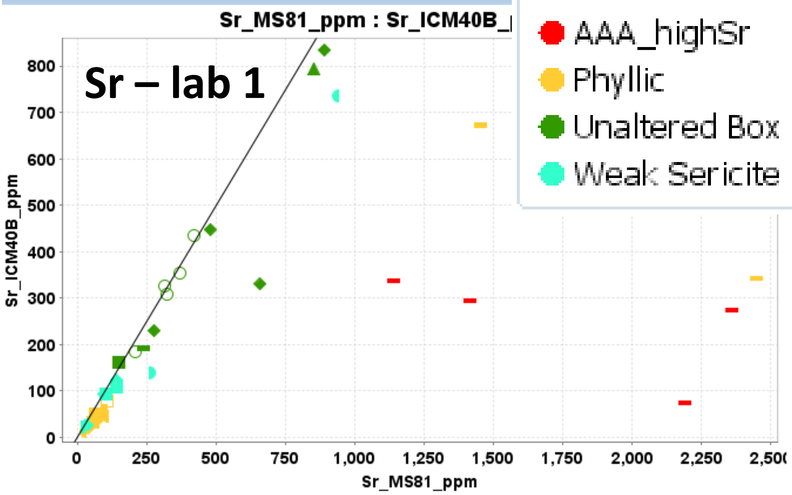
Sr_MS81_ppm : Sr_ICM40B_

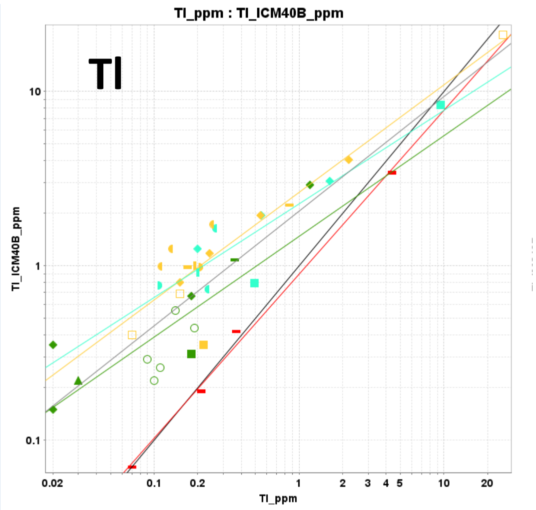
Tl_ppm : Tl_ICM40B_ppm

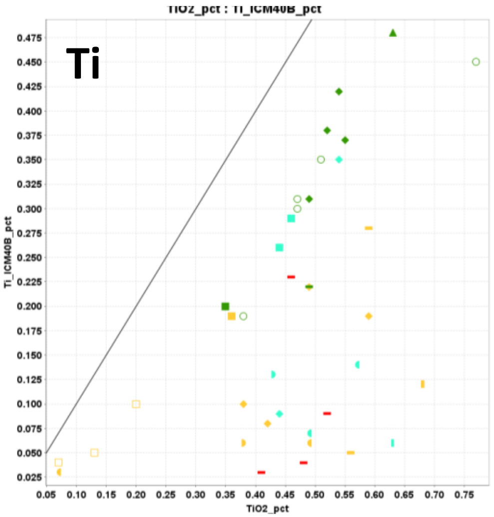
TiO2_pct : Ti_ICM40B_pct

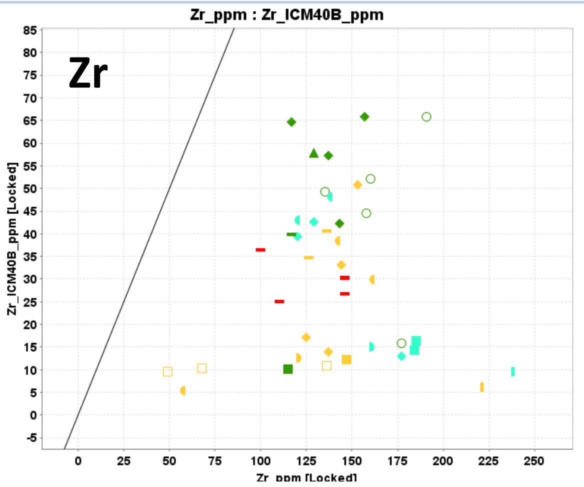
Zr_ppm : Zr_ICM40B_ppm

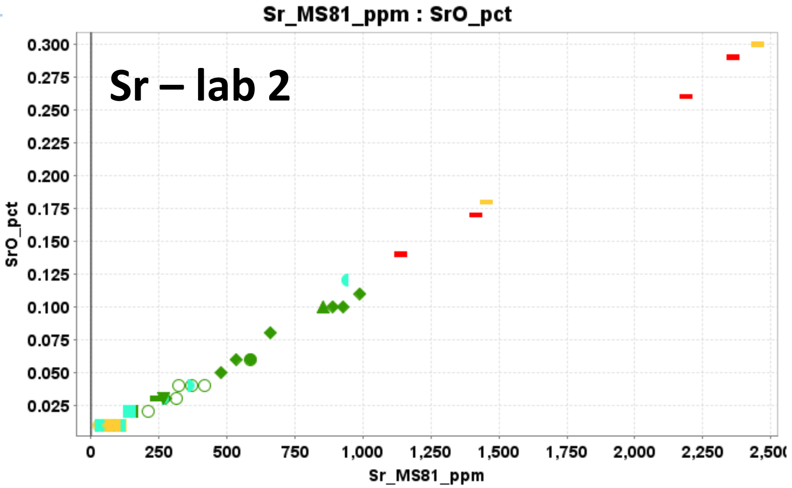
Sr_MS81_ppm : SrO_pct

- Drill core samples (whole rock) from epithermal and porphyry deposit (Bulgaria)

Analytical methodologies in exploration geochemistry

Comparison of “Supertrace” or “Ultrafine” and Classic Aqua Regia methods in soil

Approach:

- Soil samples reanalyzed by Au-supertrace method.
- This an aqua regia digest with ICP-MS finish and give a gold lower detection limit of 0.1 ppb (compared to 10-100 ppb Au in classic methods).
- Larger splits give more representative analysis of elements subject to nugget effect (e.g., Au)
- Ultrafine analysis gives better anomaly to background contrast for Au and Ag than in the classic aqua regia procedure.

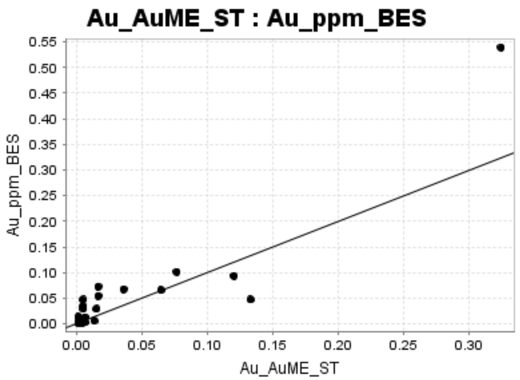
Au_AuME_ST : Au_ppm_BES

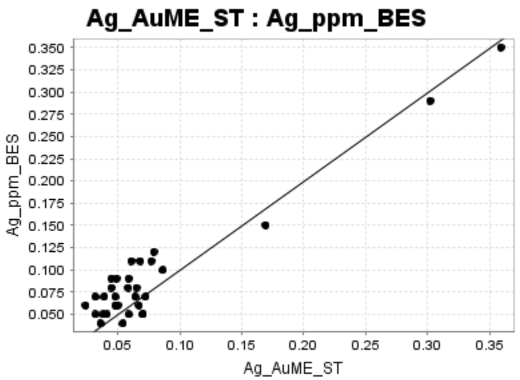
Ag_AuME_ST : Ag_ppm_BES

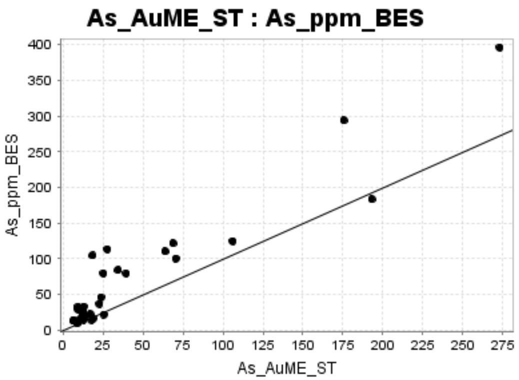
As_AuME_ST : As_ppm_BES

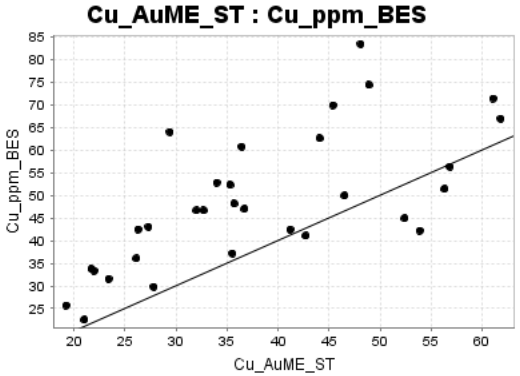
Cu_AuME_ST : Cu_ppm_BES

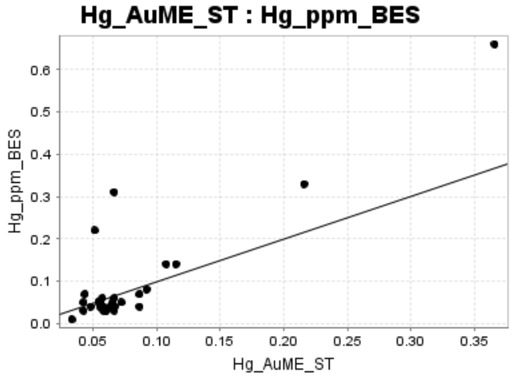
Hg_AuME_ST : Hg_ppm_BES

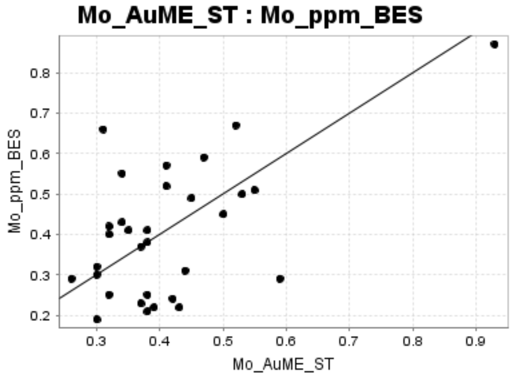
Mo_AuME_ST : Mo_ppm_BES

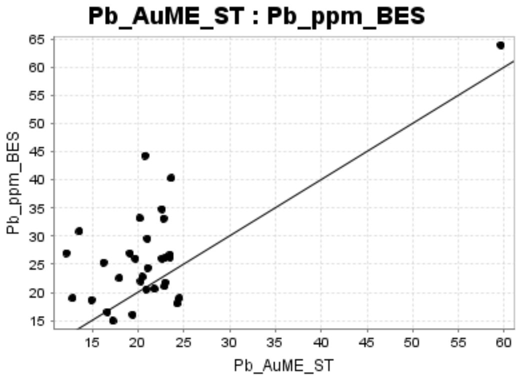
Pb_AuME_ST : Pb_ppm_BES

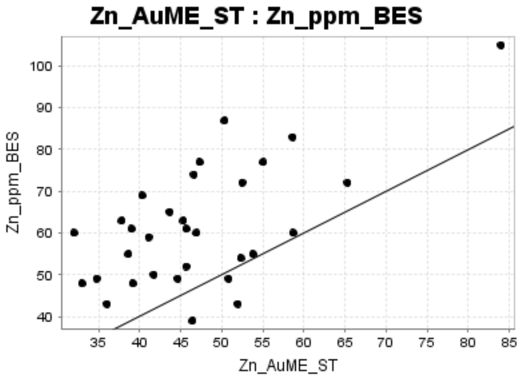
Zn_AuME_ST : Zn_ppm_BES

Supertrace on x axis

Analytical methodologies in exploration geochemistry

Comparison of “Supertrace” or “Ultrafine” and Classic Aqua Regia methods in soil

- Ultrafine analysis gives better anomaly to background contrast for Au and Ag than in the classic aqua regia procedure.
- Width of dispersion for UF and AQ is similar.
- Reproducibility of Au in ultrafine analysis is better than in normal aqua regia.

Soil Orientation Profiles for Elements Showing Response

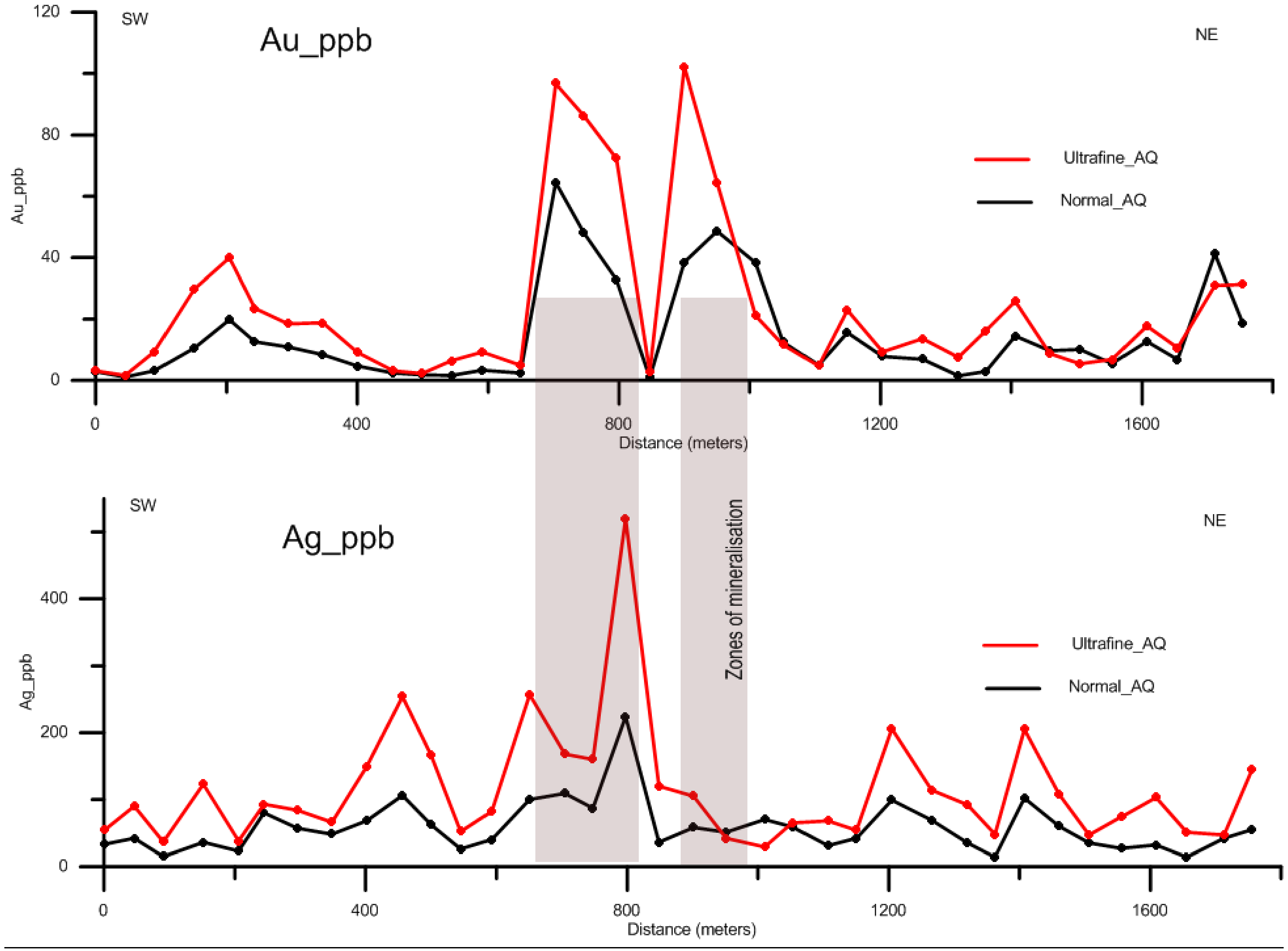

Analytical methodologies in exploration geochemistry

Example of hydroxylamine-HCl orientation work in limestone/terra rosa terrain

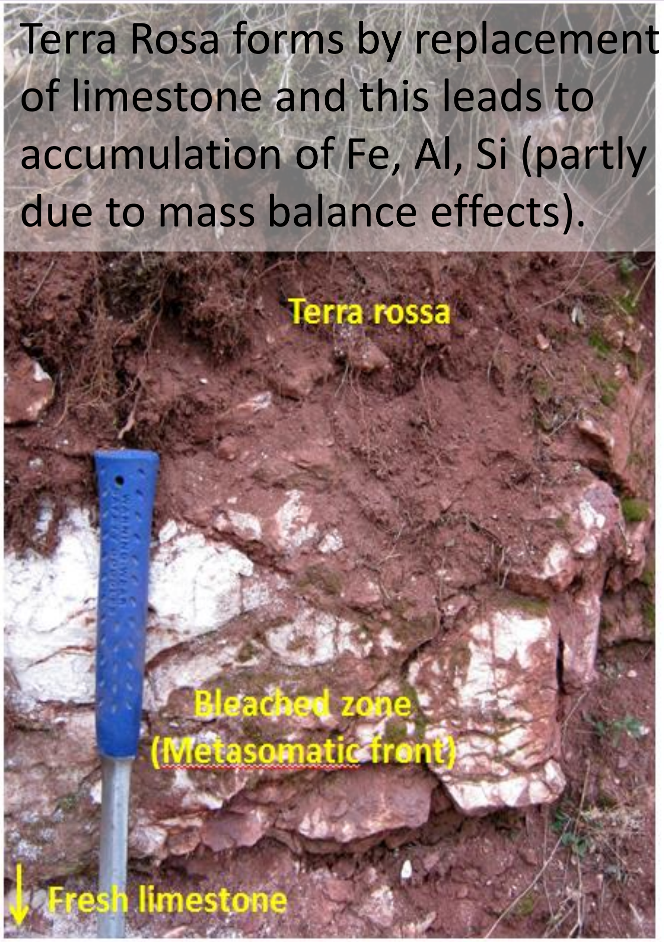

Terra Rosa forms by replacement of limestone and this leads to accumulation of Fe, Al, Si (partly due to mass balance effects).

Typical profile through the rendzina soil (terra rossa) from Umka with high Au content (>0.1 ppm) formed over a non-mineralized (<0.01 ppm) limestone bedrock.

- Can clear anomalies ("feeder zones") be identified from a comparison of hot hydroxylamine hydrochloride and aqua regia digest data?
- The existing aqua regia digest can be used as testing for crystalline Fe oxides. This analysis can be compared to the original samples from an aqua regia analysis/ICPMS.
- Dissolution is rock pH-buffer capacity dependent!

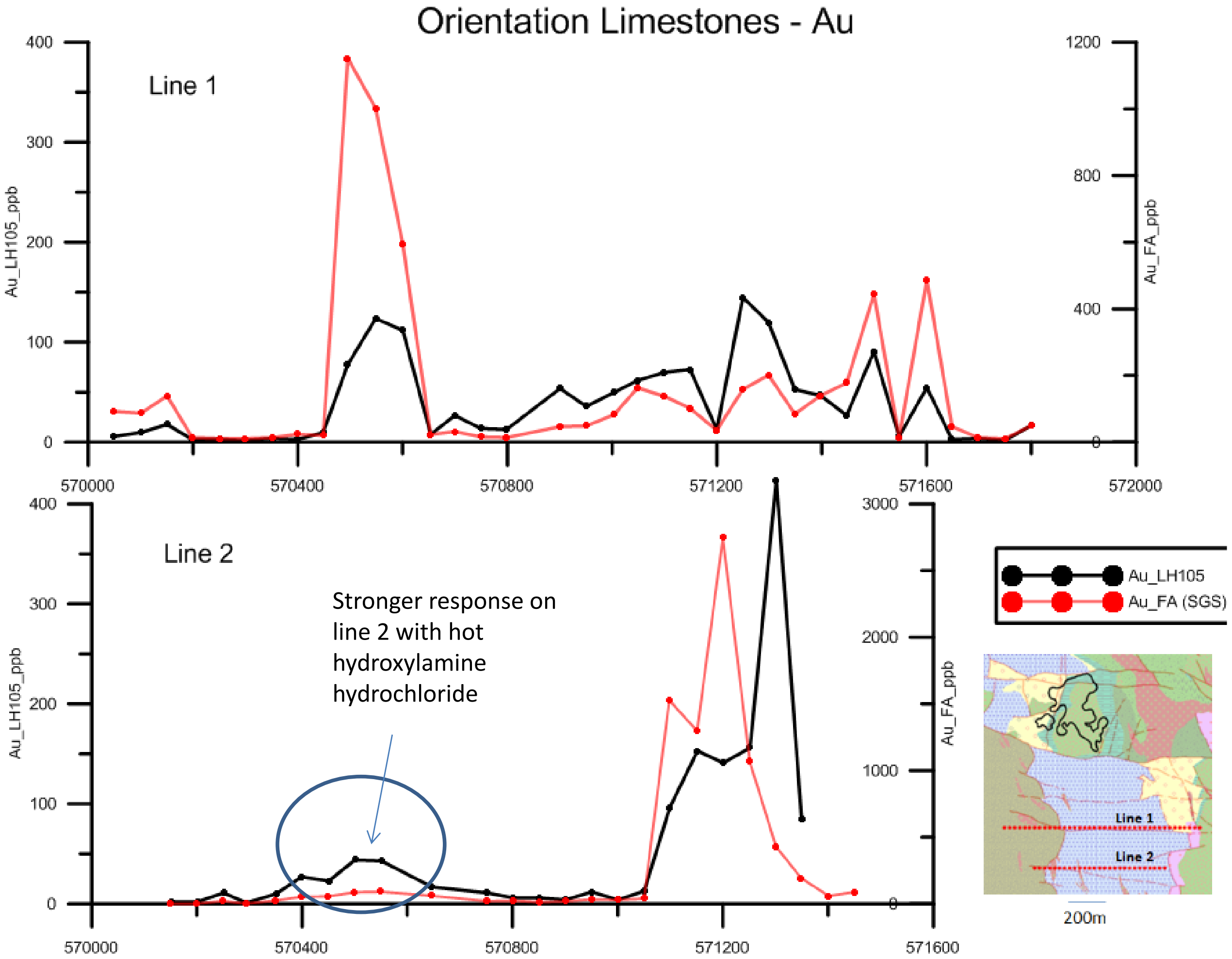

Stronger response on line 2 with hot hydroxylamine hydrochloride

Application of portable or benchtop field XRF instruments

Application of portable or benchtop field XRF instruments

Key aspects of portable XRF instruments

Typically measure 1x1 cm to a depth of ~ 2 mm in soil, especially good for heavier elements

- Need different sources for different combinations of analyte elements
- Relatively new compact detectors (e.g. HgI2, Si-PIN, Si-DRIFT and CdZnTe) are ideal for portability but their resolution is inferior to the standard Si and Ge detectors
- For important alteration light elements (i.e. Na, Mg, Si, P) need very sensible detectors and high counting times
- Use fundamental parameter method for calibration
- Very fast, non-destructive but DLs are still in the ppm range
- Accuracy (and precision) is limited by heterogeneity, moisture content, inconsistent sampling position, spectral overlap (eg Pb on As) and absorption/enhancement effects (should be taken care of by software)
- Not well established national approval/training protocols for using radiation sources in Eastern-Central Europe.

Application of portable or benchtop field XRF instruments

Portable XRF instruments – typical limits of detection

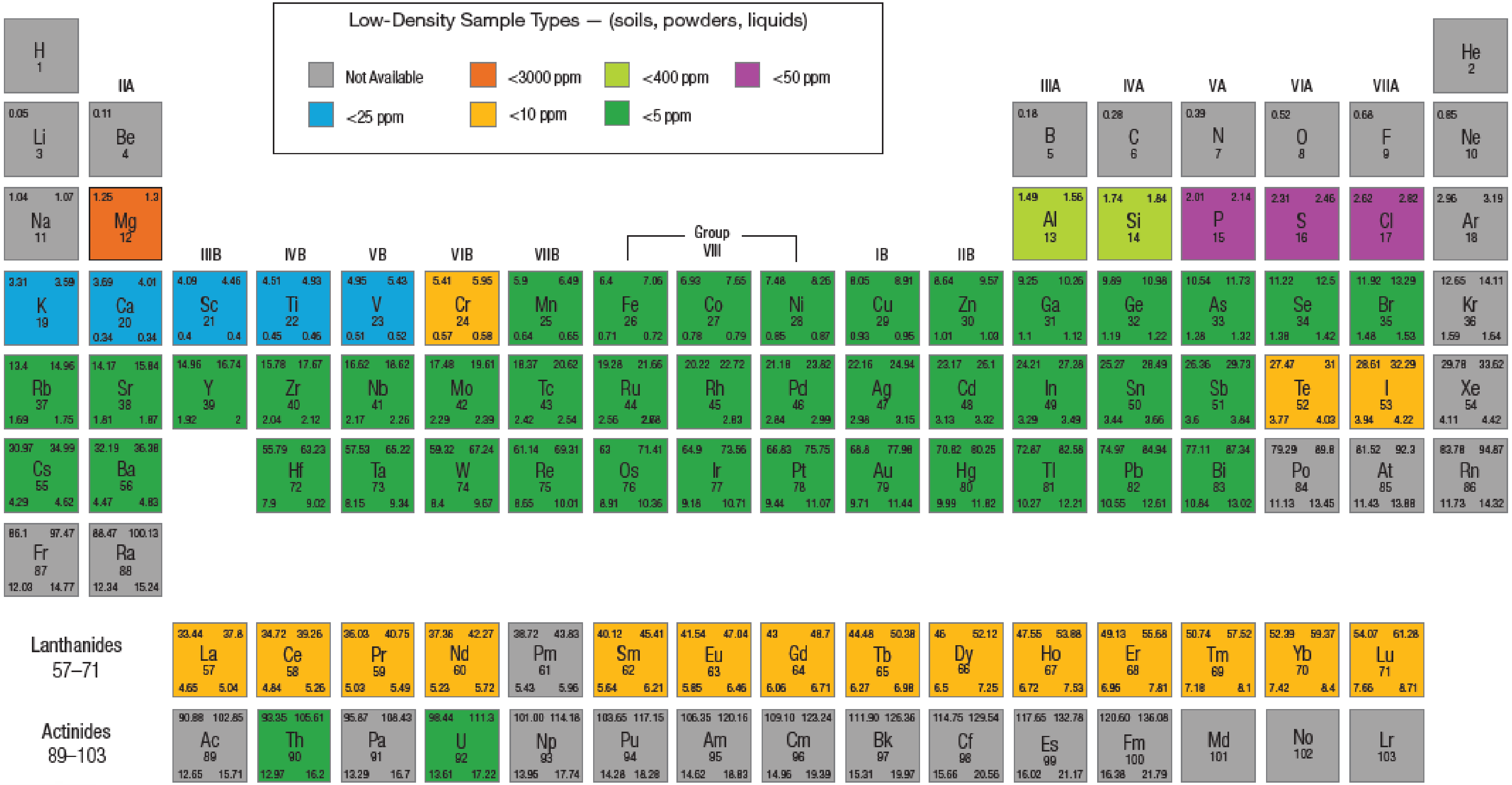

Low-Density Sample Types — (soils, powders, liquids)

⬜ Not Available 🟧 <3000 ppm 🟢 <400 ppm 🟪 <50 ppm
🟦 <25 ppm 🟨 <10 ppm 🟩 <5 ppm

	IIA	IIIB	IVB	VB	VIB	VIIB	Group VIII			IB	IIB	IIIA	IVA	VA	VIA	VIIA	
⬜ H 1																	⬜ He 2
⬜ 0.05 Li 3	⬜ 0.11 Be 4											⬜ 0.18 B 5	⬜ 0.28 C 6	⬜ 0.39 N 7	⬜ 0.52 O 8	⬜ 0.68 F 9	⬜ 0.85 Ne 10
⬜ 1.04 1.07 Na 11	🟧 1.25 1.3 Mg 12											🟢 1.49 1.56 Al 13	🟢 1.74 1.84 Si 14	🟪 2.01 2.14 P 15	🟪 2.31 2.46 S 16	🟪 2.62 2.82 Cl 17	⬜ 2.96 3.19 Ar 18
🟦 3.31 3.59 K 19	🟦 3.69 4.01 Ca 20 0.34 0.34	🟦 4.09 4.46 Sc 21 0.4 0.4	🟦 4.51 4.93 Ti 22 0.45 0.46	🟦 4.95 5.43 V 23 0.51 0.52	🟨 5.41 5.95 Cr 24 0.57 0.58	🟩 5.9 6.49 Mn 25 0.64 0.65	🟩 6.4 7.06 Fe 26 0.71 0.72	🟩 6.93 7.65 Co 27 0.78 0.79	🟩 7.48 8.26 Ni 28 0.85 0.87	🟩 8.05 8.91 Cu 29 0.93 0.95	🟩 8.64 9.57 Zn 30 1.01 1.03	🟩 9.25 10.26 Ga 31 1.1 1.12	🟩 9.89 10.98 Ge 32 1.19 1.22	🟩 10.54 11.73 As 33 1.28 1.32	🟩 11.22 12.5 Se 34 1.38 1.42	🟩 11.92 13.29 Br 35 1.48 1.53	⬜ 12.65 14.11 Kr 36 1.59 1.64
🟩 13.4 14.96 Rb 37 1.69 1.75	🟩 14.17 15.84 Sr 38 1.81 1.87	🟩 14.96 16.74 Y 39 1.92 2	🟩 15.78 17.67 Zr 40 2.04 2.12	🟩 16.62 18.62 Nb 41 2.17 2.26	🟩 17.48 19.61 Mo 42 2.29 2.39	🟩 18.37 20.62 Tc 43 2.42 2.54	🟩 19.28 21.66 Ru 44 2.56 2.68	🟩 20.22 22.72 Rh 45 2.83	🟩 21.18 23.82 Pd 46 2.84 2.99	🟩 22.16 24.94 Ag 47 2.98 3.15	🟩 23.17 26.1 Cd 48 3.13 3.32	🟩 24.21 27.28 In 49 3.29 3.49	🟩 25.27 28.49 Sn 50 3.44 3.66	🟩 26.36 29.73 Sb 51 3.6 3.84	🟨 27.47 31 Te 52 3.77 4.03	🟨 28.61 32.29 I 53 3.94 4.22	⬜ 29.78 33.62 Xe 54 4.11 4.42
🟩 30.97 34.99 Cs 55 4.29 4.62	🟩 32.19 36.38 Ba 56 4.47 4.83		🟩 55.79 63.23 Hf 72 7.9 9.02	🟩 57.53 65.22 Ta 73 8.15 9.34	🟩 59.32 67.24 W 74 8.4 9.67	🟩 61.14 69.31 Re 75 8.65 10.01	🟩 63 71.41 Os 76 8.91 10.36	🟩 64.9 73.56 Ir 77 9.18 10.71	🟩 66.83 75.75 Pt 78 9.44 11.07	🟩 68.8 77.98 Au 79 9.71 11.44	🟩 70.82 80.25 Hg 80 9.99 11.82	🟩 72.87 82.58 Tl 81 10.27 12.21	🟩 74.97 84.94 Pb 82 10.55 12.61	🟩 77.11 87.34 Bi 83 10.84 13.02	⬜ 79.29 89.8 Po 84 11.13 13.45	⬜ 81.52 92.3 At 85 11.43 13.88	⬜ 83.78 94.87 Rn 86 11.73 14.32
⬜ 86.1 97.47 Fr 87 12.03 14.77	⬜ 88.47 100.13 Ra 88 12.34 15.24																
Lanthanides 57–71		🟨 33.44 37.8 La 57 4.65 5.04	🟨 34.72 39.26 Ce 58 4.84 5.26	🟨 36.03 40.75 Pr 59 5.03 5.49	🟨 37.36 42.27 Nd 60 5.23 5.72	⬜ 38.72 43.83 Pm 61 5.43 5.96	🟨 40.12 45.41 Sm 62 5.64 6.21	🟨 41.54 47.04 Eu 63 5.85 6.46	🟨 43 48.7 Gd 64 6.06 6.71	🟨 44.48 50.38 Tb 65 6.27 6.98	🟨 46 52.12 Dy 66 6.5 7.25	🟨 47.55 53.88 Ho 67 6.72 7.53	🟨 49.13 55.68 Er 68 6.95 7.81	🟨 50.74 57.52 Tm 69 7.18 8.1	🟨 52.39 59.37 Yb 70 7.42 8.4	🟨 54.07 61.28 Lu 71 7.66 8.71	
Actinides 89–103		⬜ 90.88 102.85 Ac 89 12.65 15.71	🟩 93.35 105.61 Th 90 12.97 16.2	⬜ 95.87 108.43 Pa 91 13.29 16.7	🟩 98.44 111.3 U 92 13.61 17.22	⬜ 101.00 114.18 Np 93 13.95 17.74	⬜ 103.65 117.15 Pu 94 14.28 18.28	⬜ 106.35 120.16 Am 95 14.62 18.83	⬜ 109.10 123.24 Cm 96 14.96 19.39	⬜ 111.90 126.36 Bk 97 15.31 19.97	⬜ 114.75 129.54 Cf 98 15.66 20.56	⬜ 117.65 132.78 Es 99 16.02 21.17	⬜ 120.60 136.08 Fm 100 16.38 21.79	⬜ Md 101	⬜ No 102	⬜ Lr 103	

Application of portable or benchtop field XRF instruments

Calibration of beam vs. element suite vs. analytical time

Parallel Coordinate Plot showing resolution of instrument at various beam counting time setups (copper-gold mineralized sample, Bulgaria)

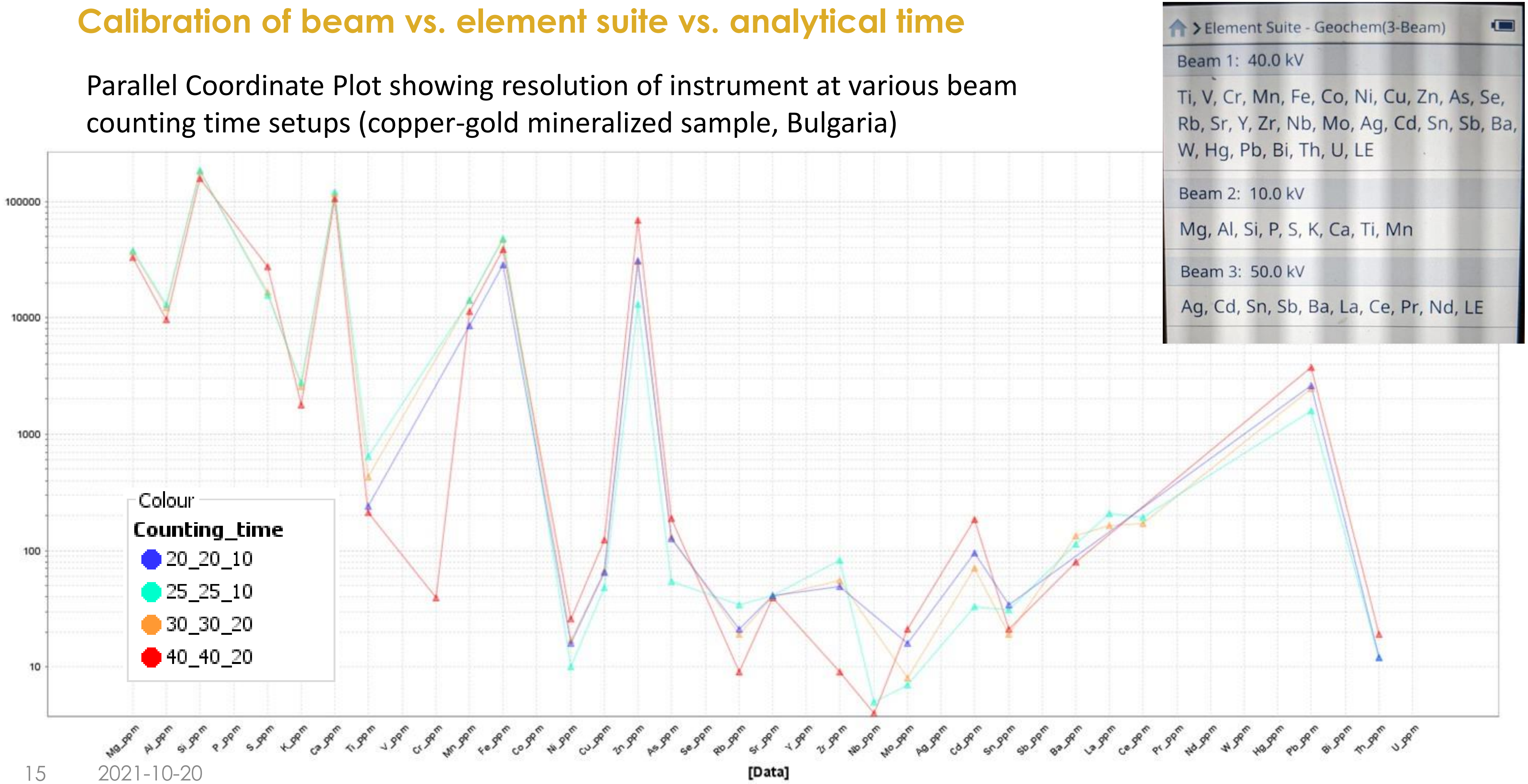

> Element Suite - Geochem(3-Beam)

Beam 1: 40.0 kV

Ti, V, Cr, Mn, Fe, Co, Ni, Cu, Zn, As, Se, Rb, Sr, Y, Zr, Nb, Mo, Ag, Cd, Sn, Sb, Ba, W, Hg, Pb, Bi, Th, U, LE

Beam 2: 10.0 kV

Mg, Al, Si, P, S, K, Ca, Ti, Mn

Beam 3: 50.0 kV

Ag, Cd, Sn, Sb, Ba, La, Ce, Pr, Nd, LE

pXRF integration in drill core logging and mapping

- Drill core striplog with one point pXRF measurement/ 1 meter distance in epithermal Au-Ag-Pb-Zn and porphyry Au-Cu mineralized section.

- pXRF data defines well mineralized zones, alteration footprints and lithology changes.

- Helps on real time follow-up of drilling intersects and fast/cost-effective decision on drilling plans (1 meter of drilling cost >200 Euro and it produce 50-100m core/day, no time to wait for laboratory results)

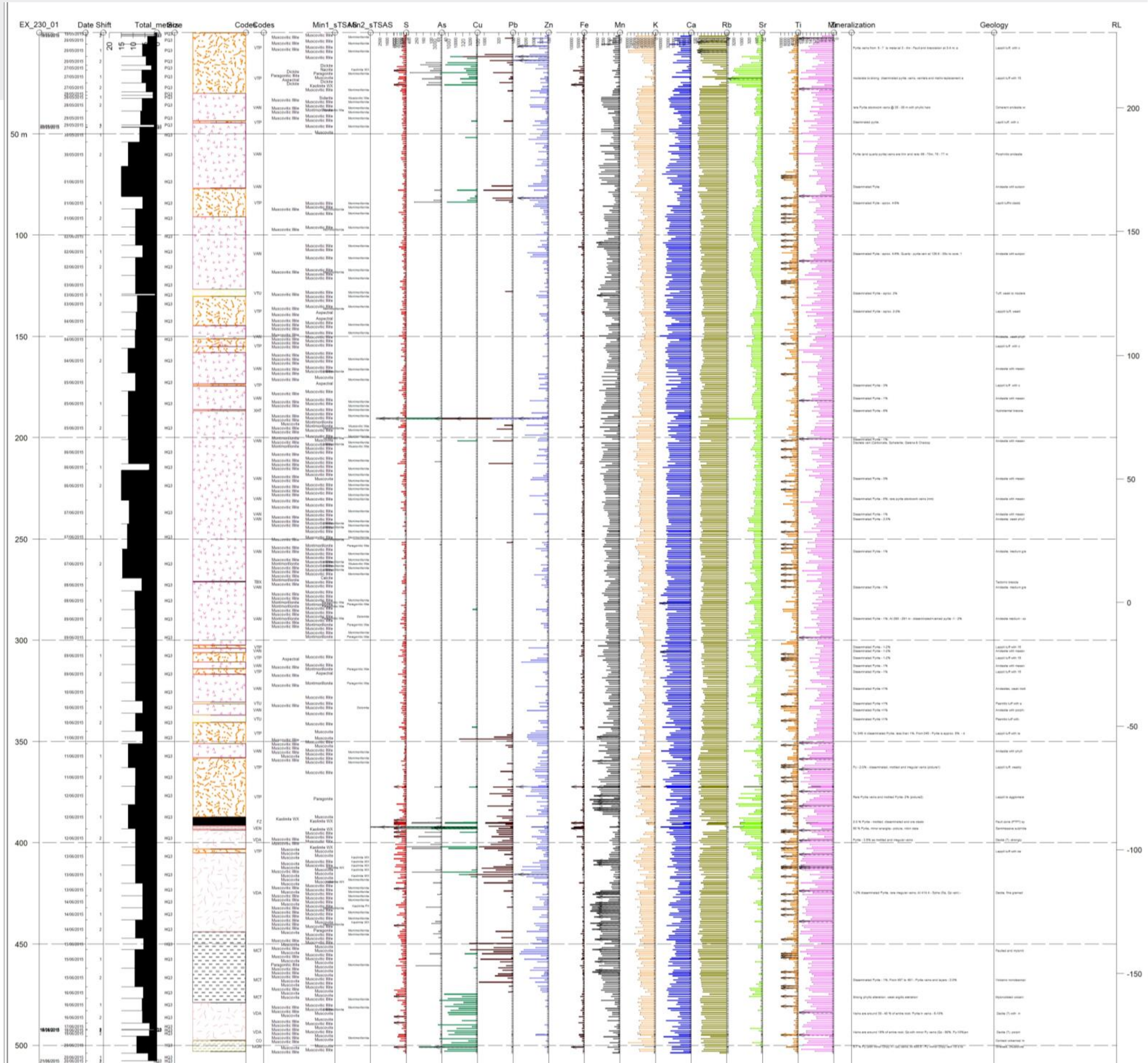

Application of portable or benchtop field XRF instruments

Comparison of various pXRF and laboratory measurements (accuracy, precision, matrix effect)

- Most alteration and mineralization related elements (As, Cu, Pb, Zn, S, Sr, Rb) show good linear correlation in the case of pXRF pulp data when is compared to regular 4 acid ICP-MS dataset;
- Point like drill core pXRF measurements show higher variability compared to pulp pXRF measurements, which suggest that the studied elements are hosted in less homogenously distributed (alteration) minerals (vein zones vs. impregnations).

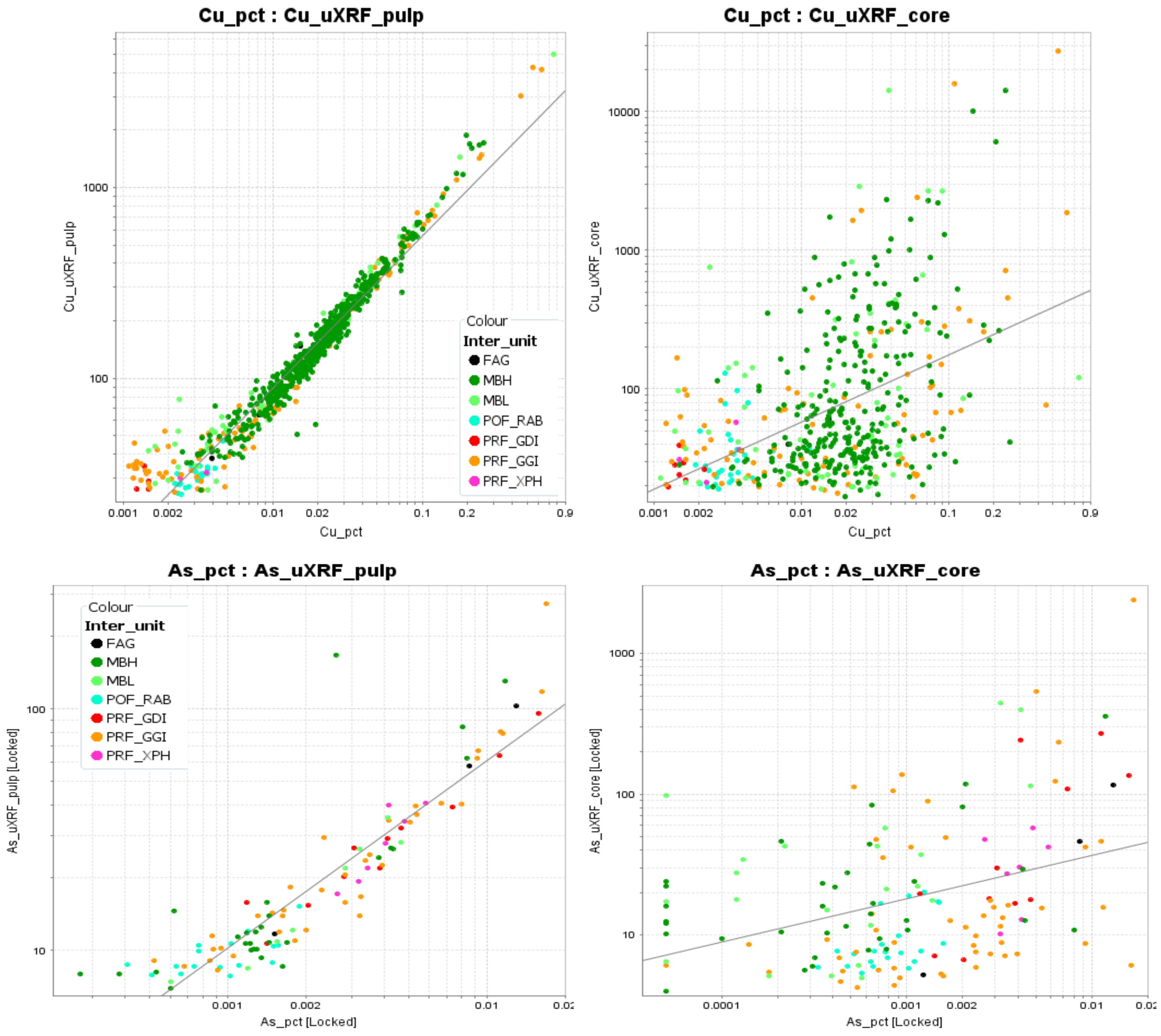

Application of portable or benchtop field XRF instruments

Comparison of various pXRF and laboratory measurements (accuracy, precision, matrix effect)

- In several metamorphic basement and granodiorite samples Ca and Mn show higher values using µXRD, which suggest the presence of garnet as undissolved mineral by 4 acid leaching.

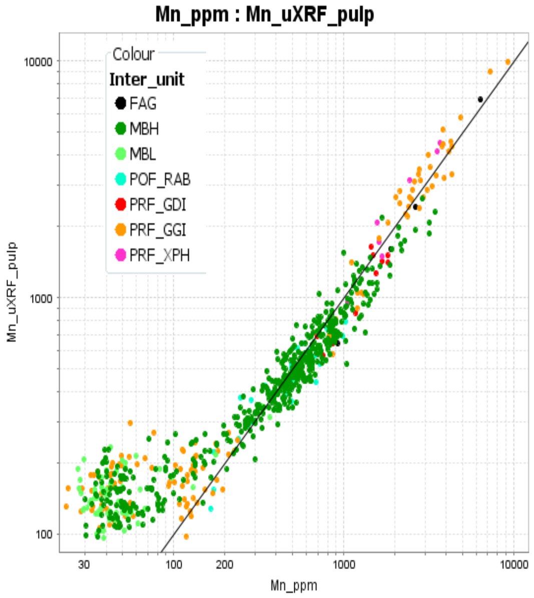

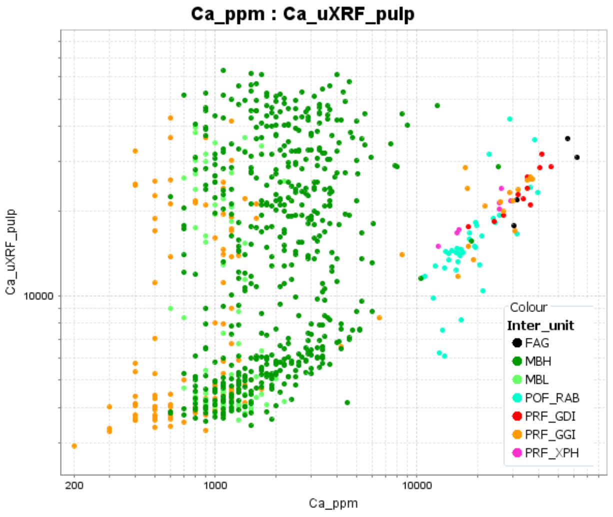

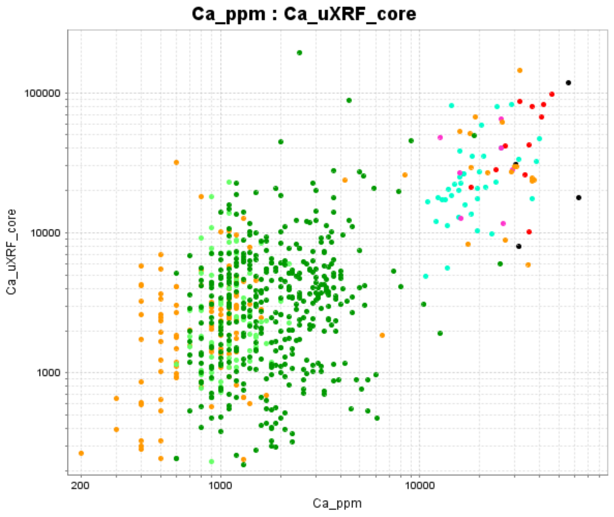

Application of portable or benchtop field XRF instruments

Comparison of various pXRF and laboratory measurements (accuracy, precision, matrix effect)

- K assays show weak correlation – it is unclear this relationship; it might be related to dissolution problems of illite/muscovite in the laboratory assays

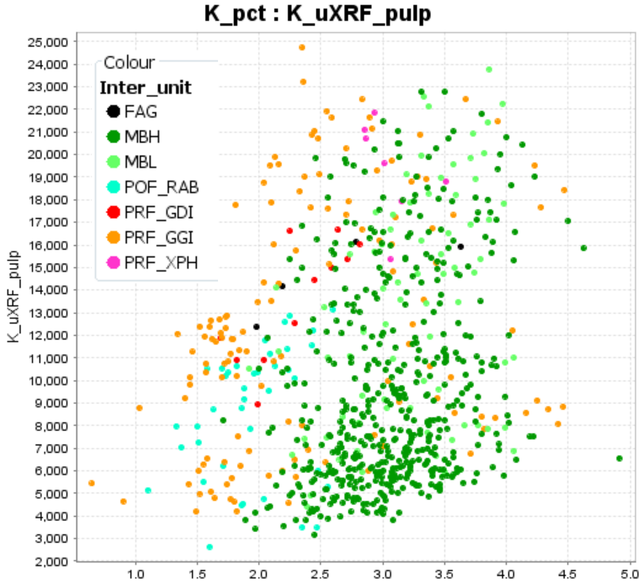
K_pct : K_uXRF_pulp

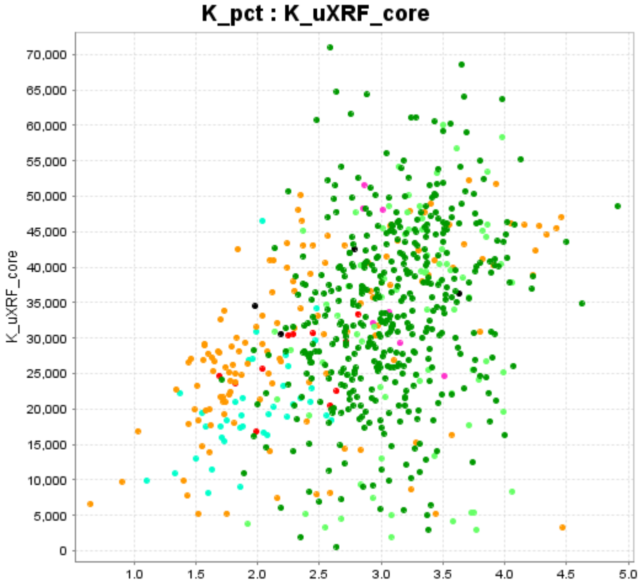
K_pct : K_uXRF_core

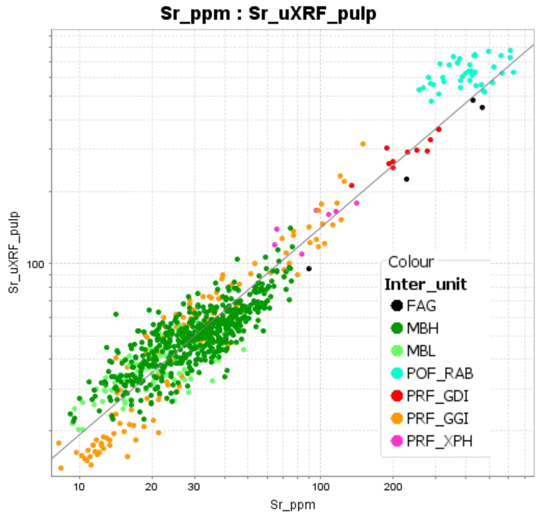
Sr_ppm : Sr_uXRF_pulp

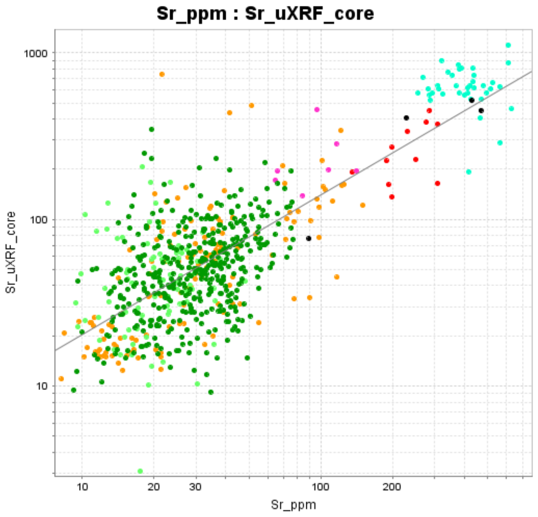
Sr_ppm : Sr_uXRF_core

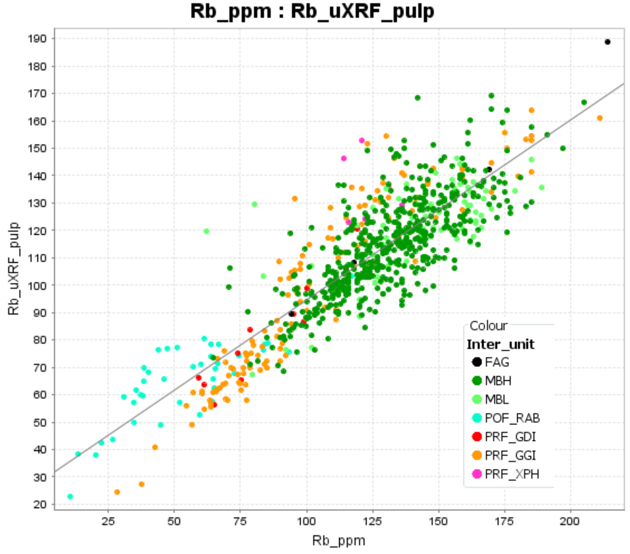
Rb_ppm : Rb_uXRF_pulp

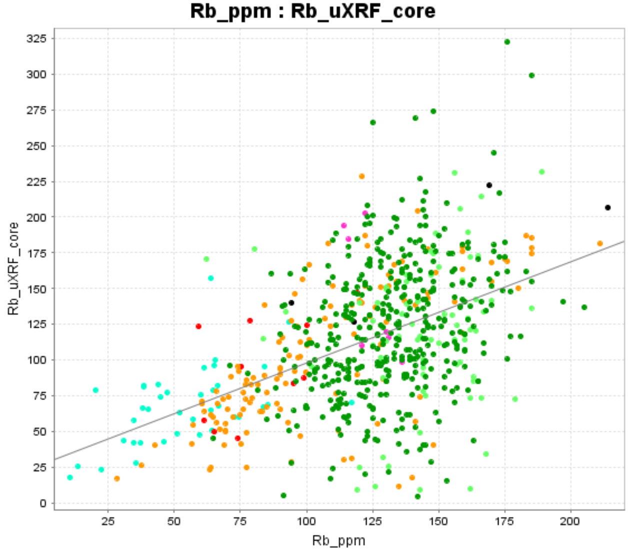
Rb_ppm : Rb_uXRF_core

Application of portable or benchtop field XRF instruments

Comparison of various pXRF and laboratory measurements (accuracy, precision, matrix effect)

- Elements (Ti, Zr) hosted by sparsely distributed accessory and refractory (in 4 acid solution) minerals show very weak correlation in both µXRD and 4 acid MS dataset. For these elements the µXRD measurements on pulp samples provide better resolution, therefore rock type identification (diorite vs. granodiorite) could be more effective when using µXRD assays from pulp samples.
- Zr-Ti discrimination proposed using 4 acid data from quartz-diorite and diorite is not confirmed by µXRD results.

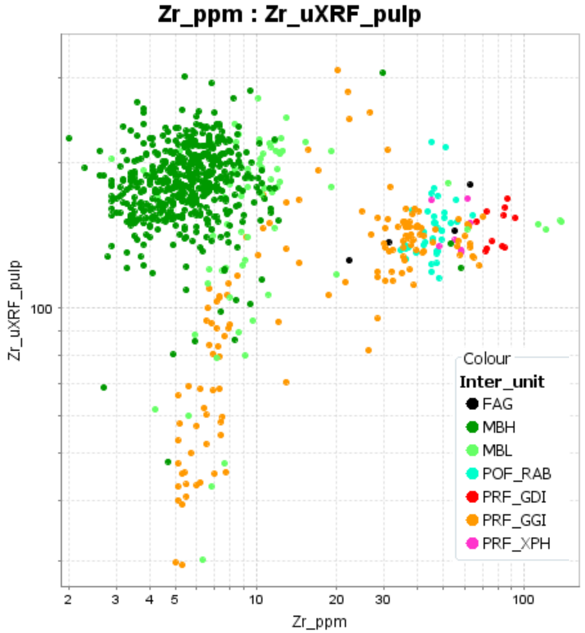
Zr_ppm : Zr_uXRF_pulp

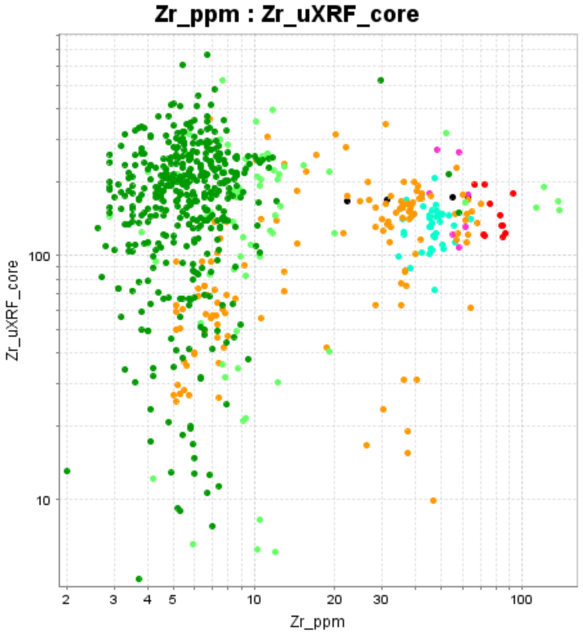
Zr_ppm : Zr_uXRF_core

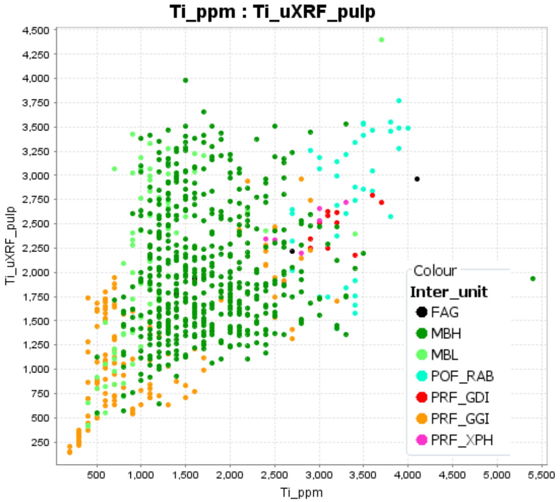
Ti_ppm : Ti_uXRF_pulp

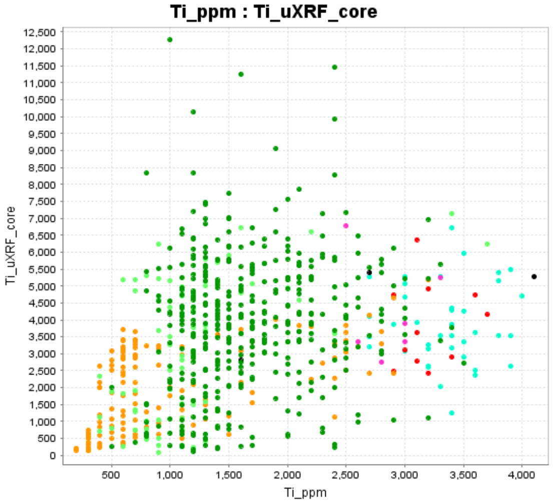
Ti_ppm : Ti_uXRF_core

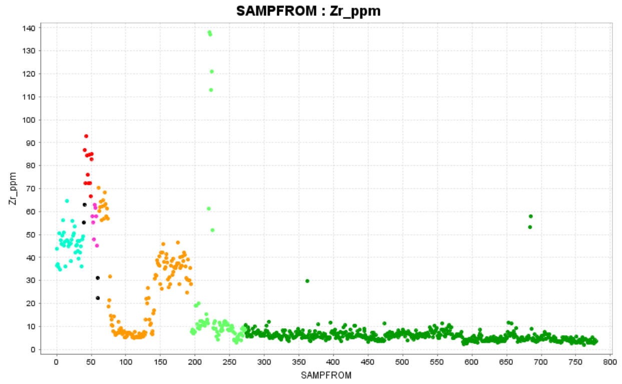
SAMPFROM : Zr_ppm

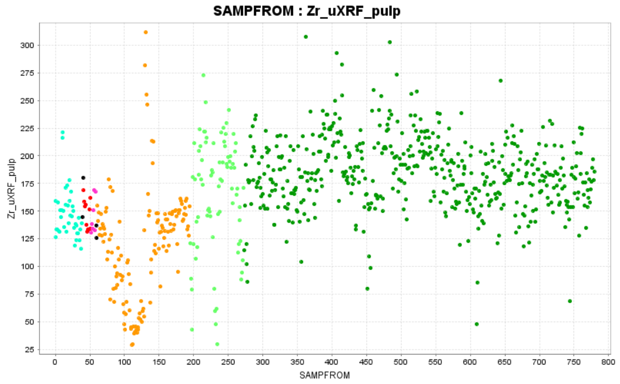
SAMPFROM : Zr_uXRF_pulp

VNIR-SWIR spectroscopy (portable and core scan)

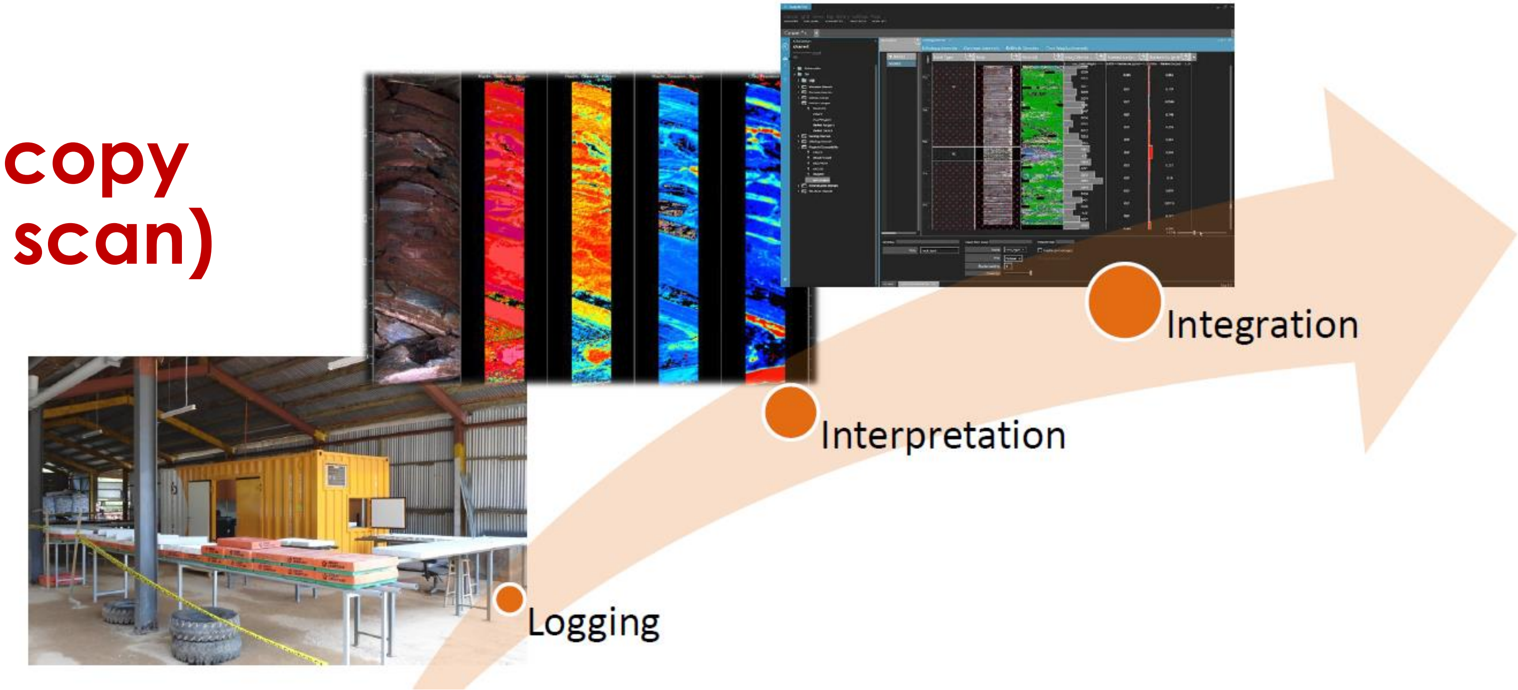

VNIR-SWIR spectroscopy (portable and core scan)

Spectral signatures/reflectance of key minerals

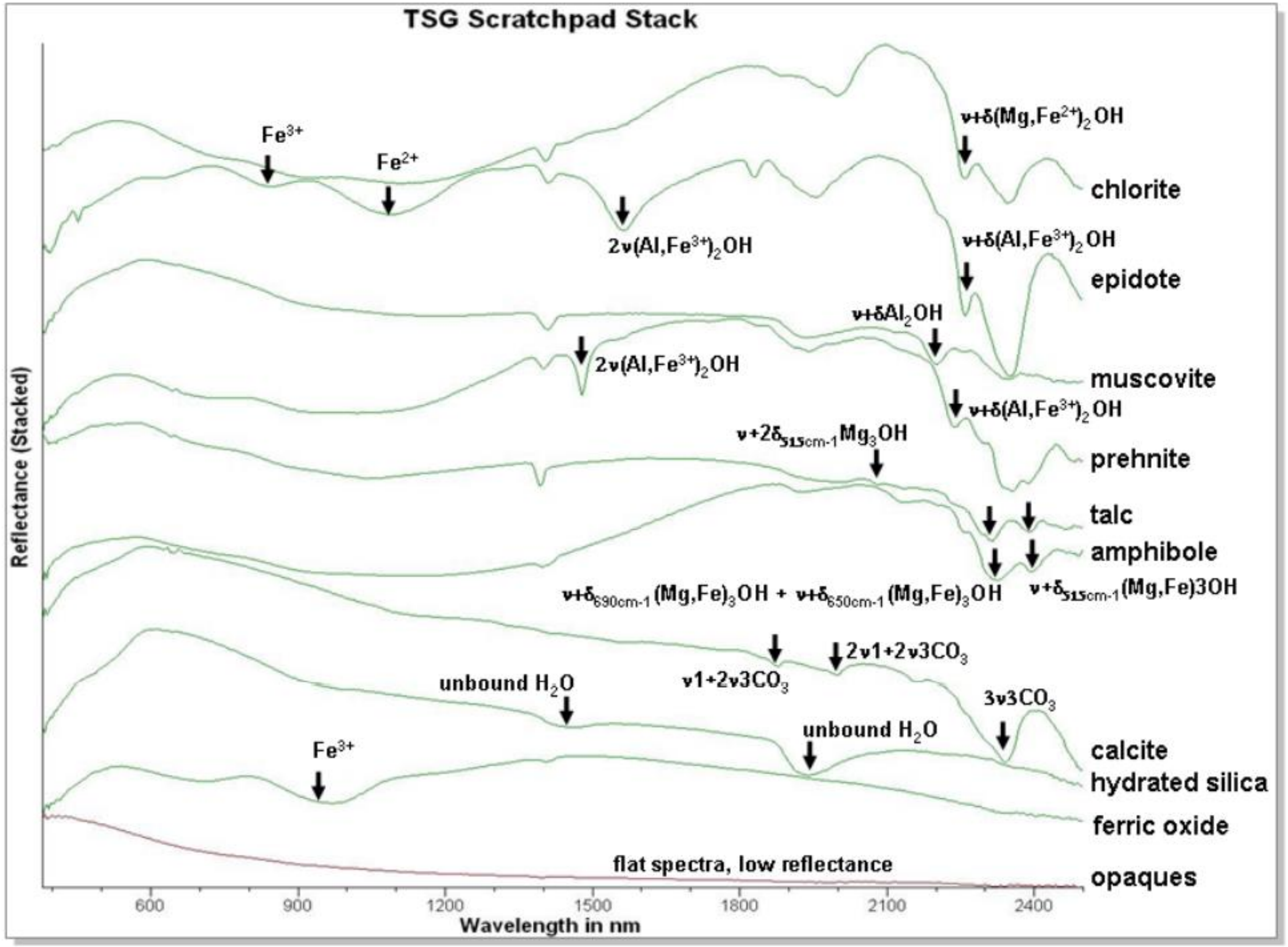

- Each alteration mineral has a distinctive spectral signature/reflectance, composed of several absorption features (width, depth), which is a function of composition, crystallinity, concentration, water content and environmental considerations.
- SWIR spectrally active minerals: phyllosilicates, sulphates, carbonates
- Not just mineral identification, temperature and pH indicator about formation of muscovite, clays and APS minerals.

VNIR-SWIR spectroscopy (portable and core scan)

Core scanning benefits

- An automated core logging (mineralogy mapping) solution – an objective, repeatable, quantitative, scalable method;
- Provides photographic records to compliment the electronic mineralogy maps;
- Maps subtle mineralogical, alteration, structural and compositional changes to better understand the geology / history / paragenesis of the deposit – possible additional knowledge for vectors to mineralisation;
- High sample and spatial resolution can be integrated into detailed block models / 3d mineralogy;
- Better mineralogy improves metallurgical and geotechnical understandings (resource estimation) – note the involvement of other departments in the implementation of this tool;
- High sample and spatial resolution can be integrated into detailed block models / 3d mineralogy;
- Electronic core libraries – permanent records provide protection for a key asset;
- Electronic records allow core to be re-logged or re-processed and quickly disseminate results companywide (web-based core library);
- A modern approach to core logging and a competitive advantage across both exploration and mining activities.

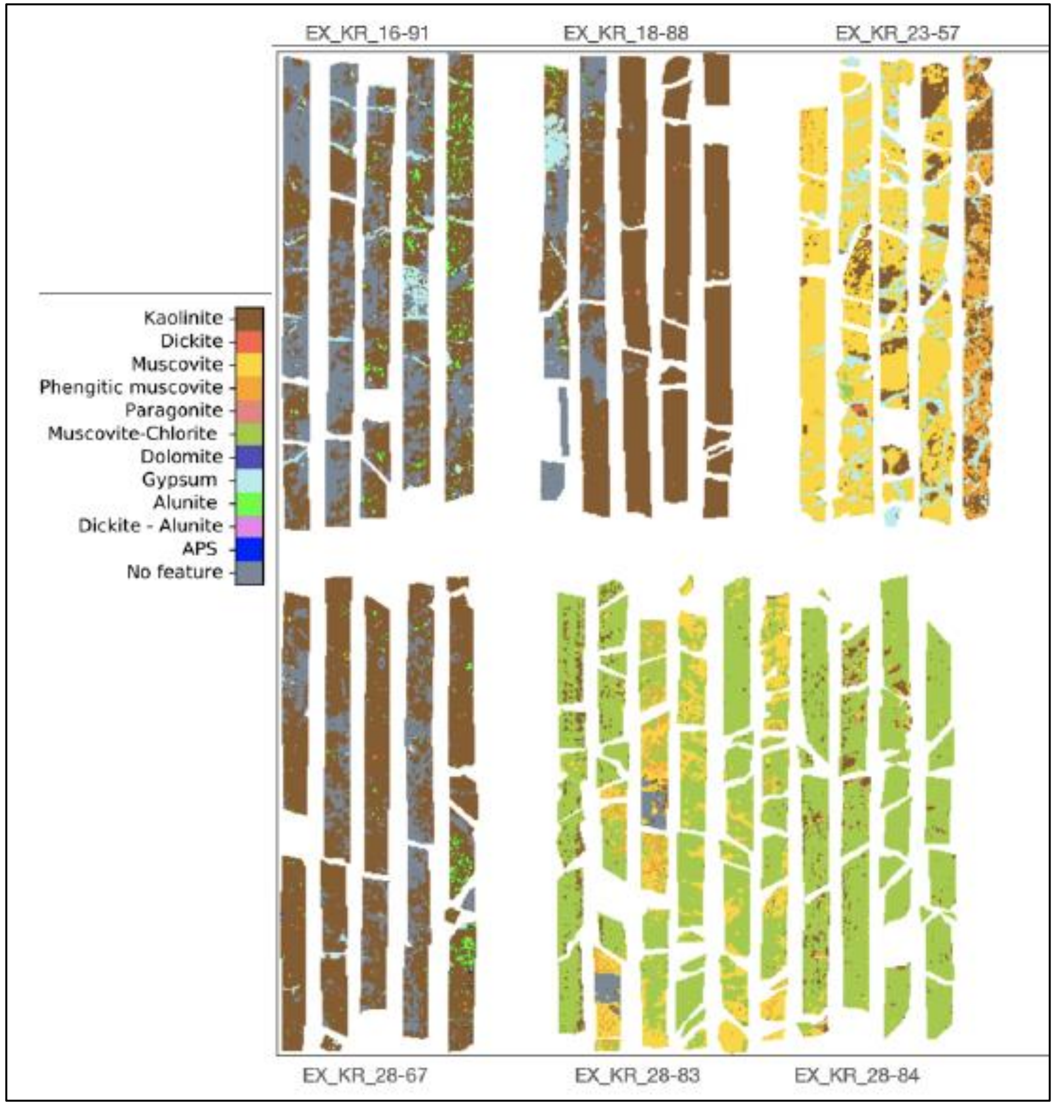

VNIR-SWIR spectroscopy (portable and core scan)

Examples: SWIR spectral endmembers/features

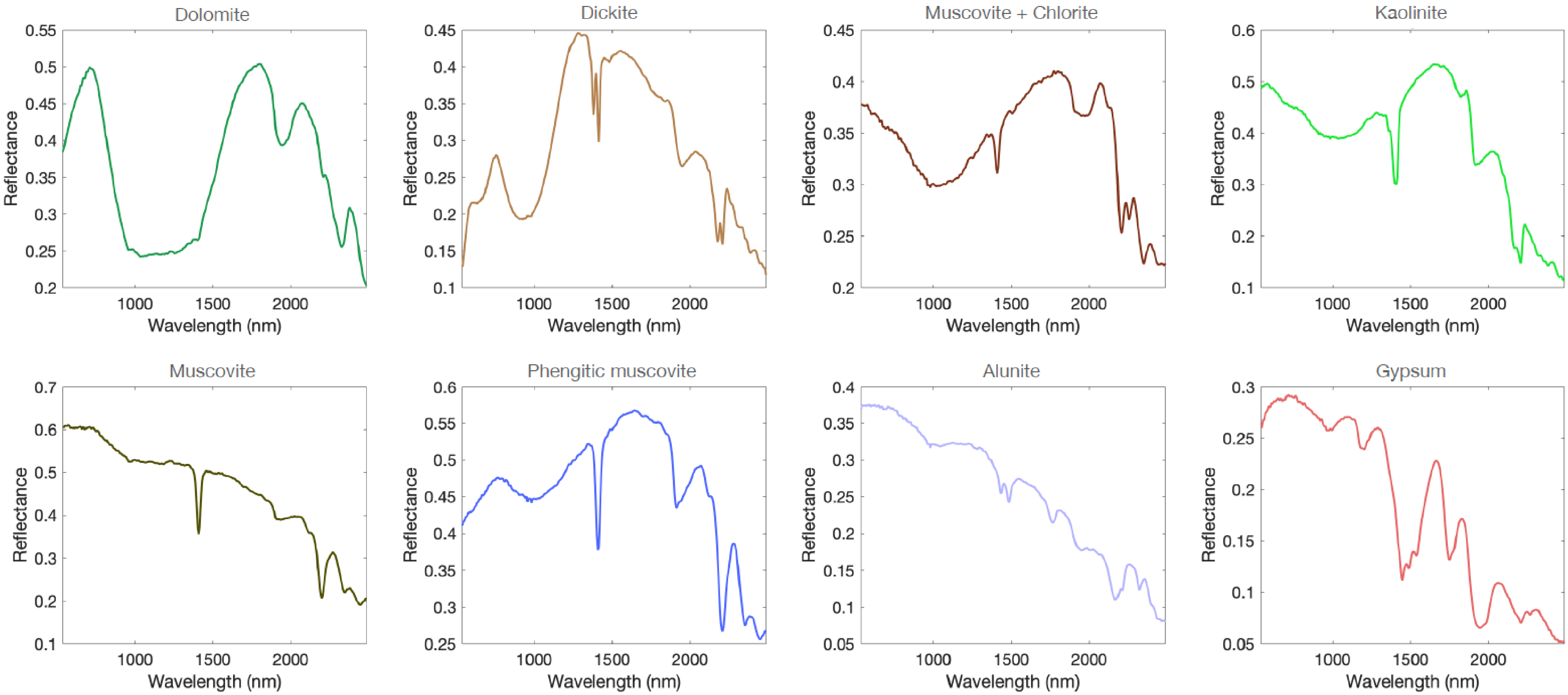

VNIR-SWIR spectroscopy (portable and core scan)

Core scanning: typical camera functions and interpretation processes

- VNIR, visible and near infrared: 400-1000 nm (for detecting heavy minerals, sulphides);
- SWIR, short-wave infrared, 1000-2500 nm (for detecting alteration minerals);
- LWIR, long-wave infrared or thermal infrared: ~8 – 12 microns (useful range for detecting many major minerals);
- High-resolution RGB for visual, photographic images of the core;
- 3D core profiler @ 0.015mm (15 micron) height resolution.

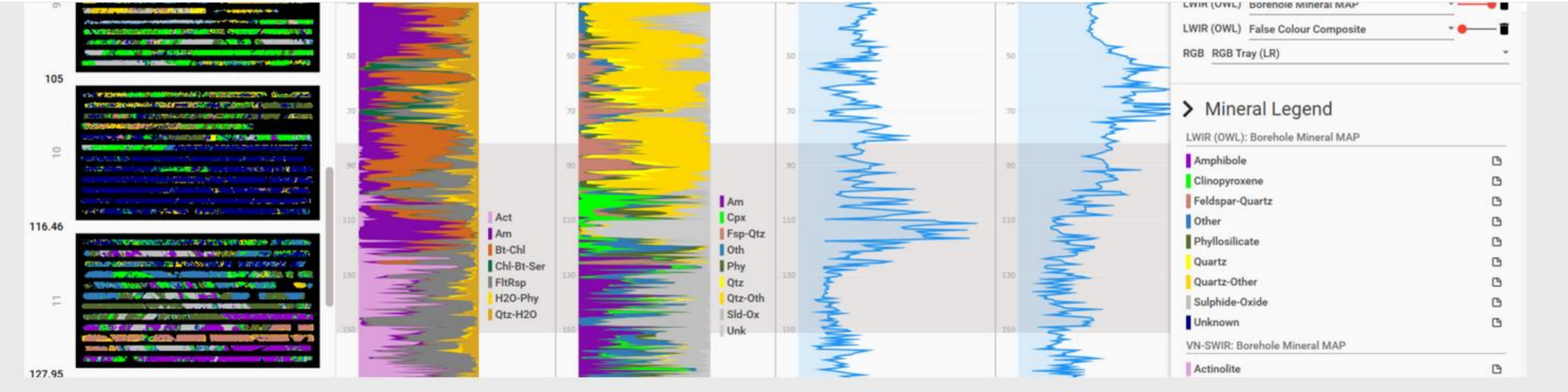

- Mineral maps that display the textural relationships of the minerals in a core and distinguish subtle variations in mineral composition with depth, including carbonates and clay species.
- Curves of mineralogical and textural data that can be imported into any log software or modeling program.
- Access to both raw spectral data and their hyperspectral interpretation via web-based platforms that enables clients to view, interrogate and integrate their spectral data.

VNIR-SWIR spectroscopy (portable and core scan)

Examples: Absorption features by position in the range between 1370 - 1660 nm, the extracted spectral features combined into a mineral map for the drill-cores

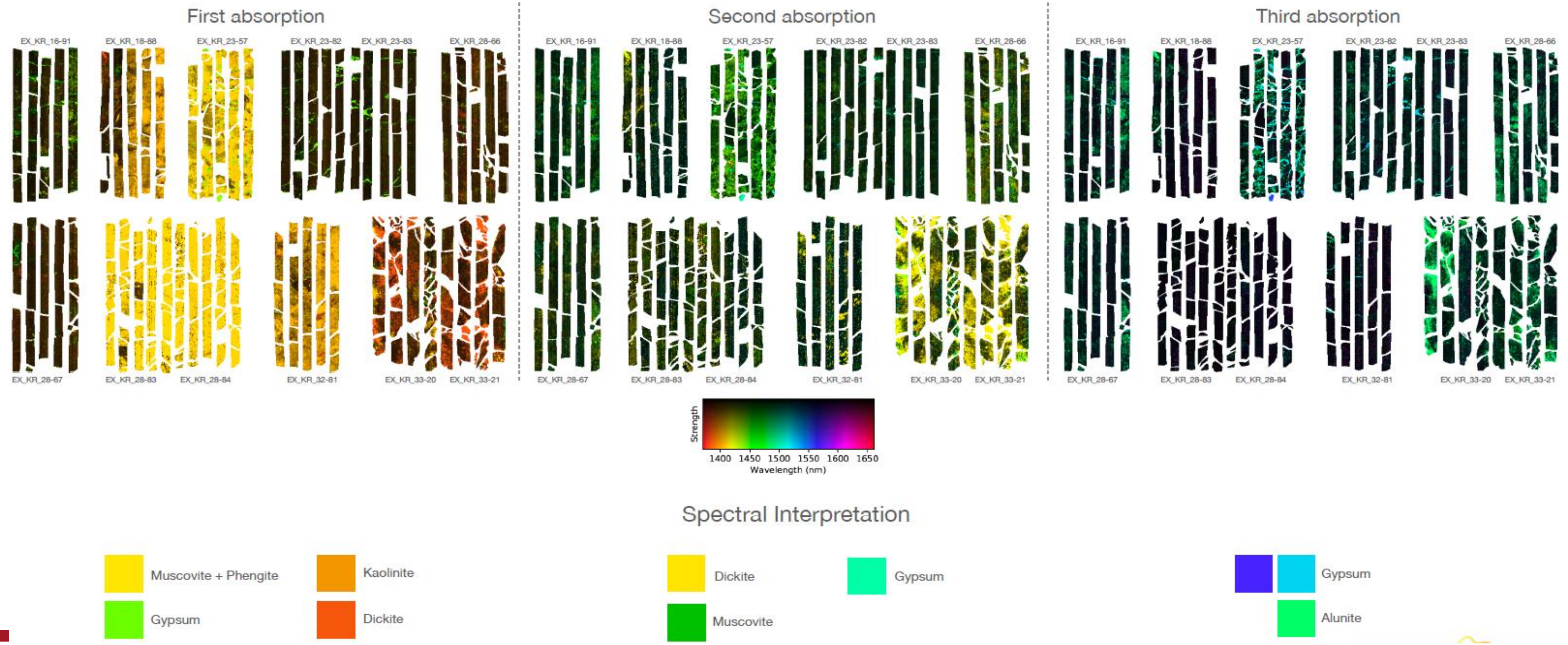

VNIR-SWIR spectroscopy (portable and core scan)

Examples: SWIR and LWIR dominant mineral map using SOM (self-organized method) logs compared to lithology logging, and Au and As assay data

- **LWIR data** marks well the sediment and hydrothermal breccia contact by orthoclase-quartz vs only quartz paragenesis. Additionally, dolomite only occur in the sandstones.
- **SWIR data** suggest strong illite-smectite and weak kaolinite? alteration associated to the Au-As enrichment. Gypsum and smectite occurs in the hanging-wall zone, while chlorite in the footwall zone.

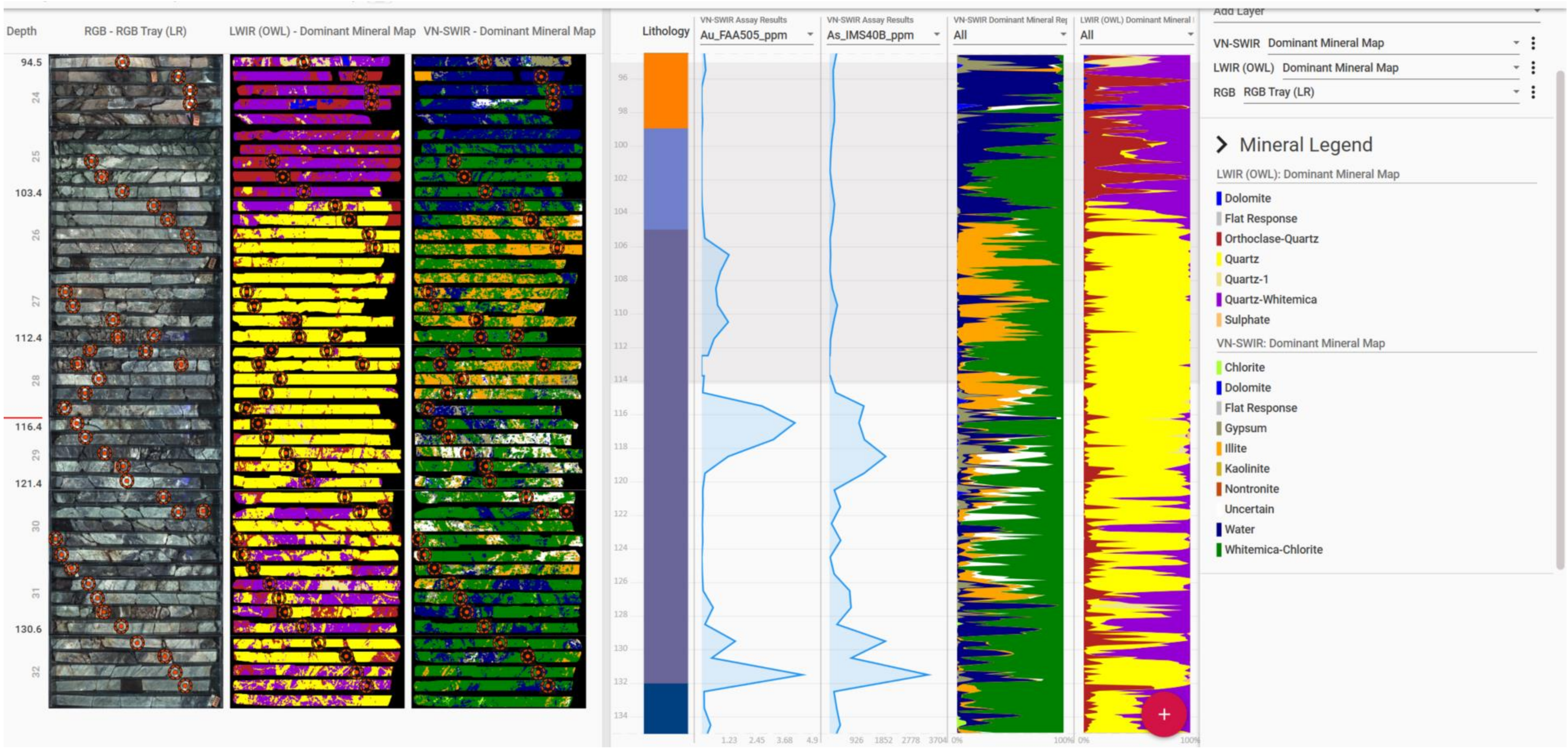

Au_FAA505_ppm
As_IMS40B_ppm
All
All

VN-SWIR Dominant Mineral Map
LWIR (OWL) Dominant Mineral Map
RGB RGB Tray (LR)

Mineral Legend

LWIR (OWL): Dominant Mineral Map

- Dolomite
- Flat Response
- Orthoclase-Quartz
- Quartz
- Quartz-1
- Quartz-Whitemica
- Sulphate

VN-SWIR: Dominant Mineral Map

- Chlorite
- Dolomite
- Flat Response
- Gypsum
- Illite
- Kaolinite
- Nontronite
- Uncertain
- Water
- Whitemica-Chlorite

VNIR-SWIR spectroscopy (portable and core scan)

Examples: SWIR data – Dominant Mineral Map interpreted by spectral geologist and spectral indices

Smectite vs. illite distribution:

- **H2O-AlOH index** is the ratio between D1950 and D2200, and provides a simpler means of evaluating bound water content within aluminous phyllosilicates. >3 records the presence of smectite, <3 and >0.5 is an indication of the presence of illite with varying degrees of smectite-illite interlayering. Proxy for temperature.
- **Ser_XT01 index** record the width of the Al-OH absorption, higher values for this index record lower crystallinity, so smectitic clays will be highest, followed by illite-smectite, illite, and finally muscovite.

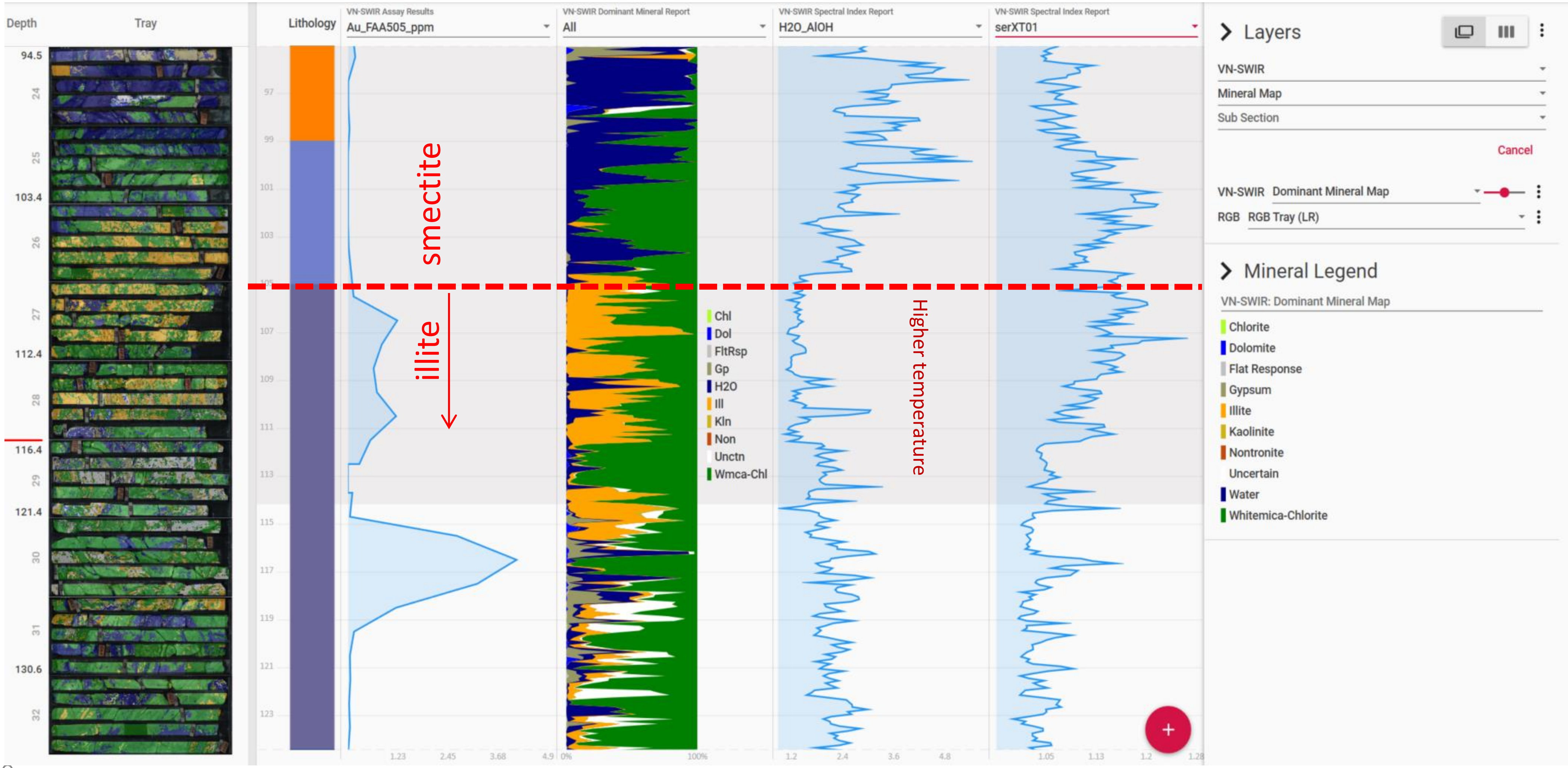

VNIR-SWIR spectroscopy (portable and core scan)

Examples: Kaolinite abundance and crystallinity

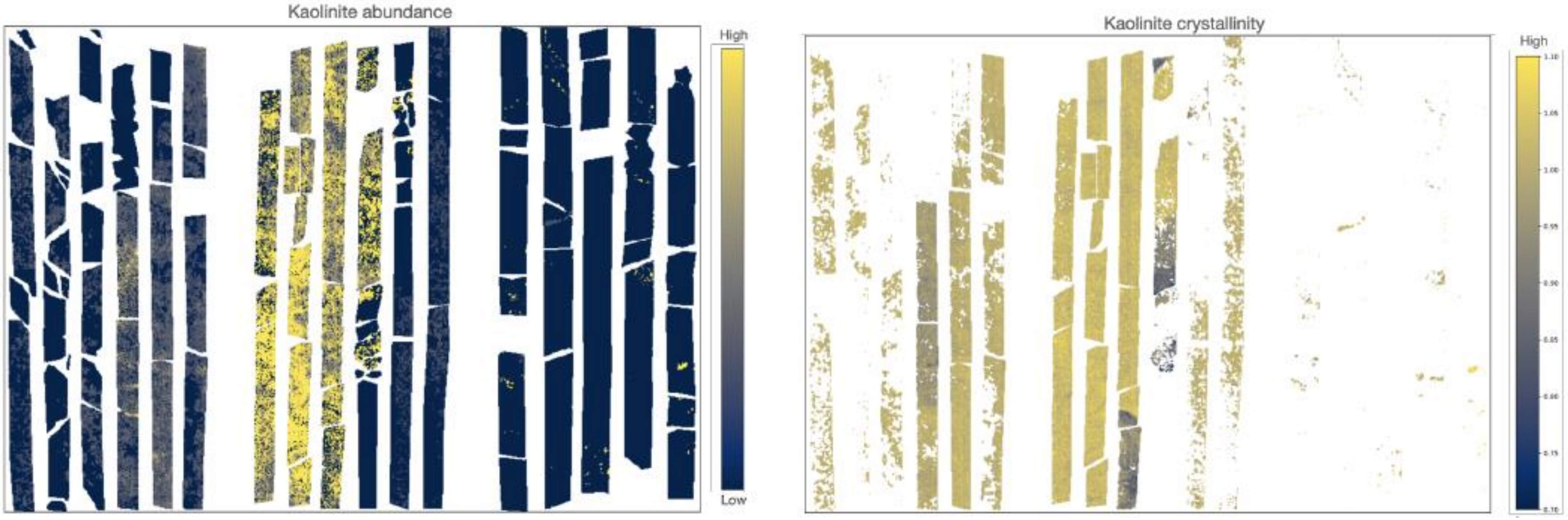

Spectral indices plots highlighting the abundance of the kaolinite (left)) and its crystallinity (right) for drill cores from epithermal mineralization.

Tripod- and UAV-based Hypercloud Spectral Mapping of Pit Walls and Outcrops

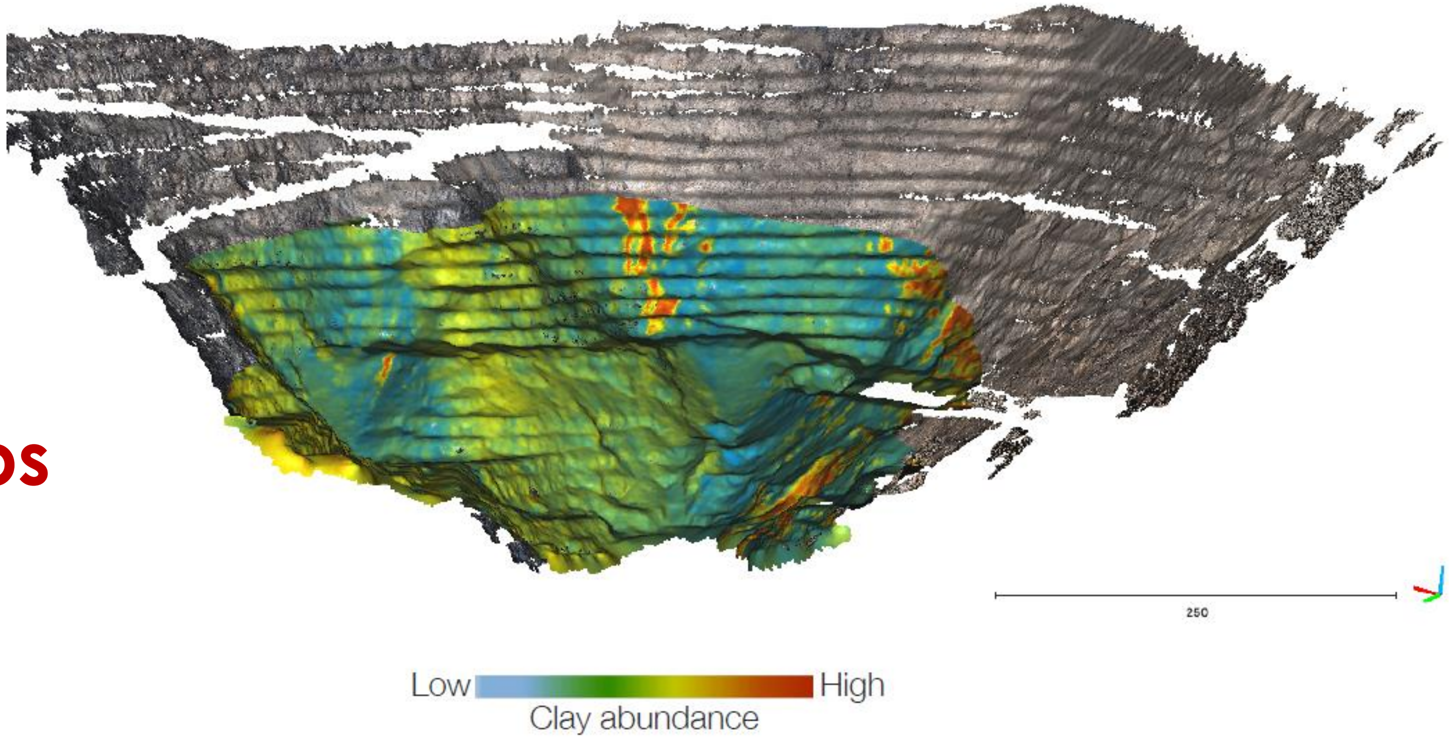

Tripod- and UAV-based Hypercloud Spectral Mapping of Pit Walls and Outcrops

Preprocessing workflow (based on SWIR and VNIR sensors)

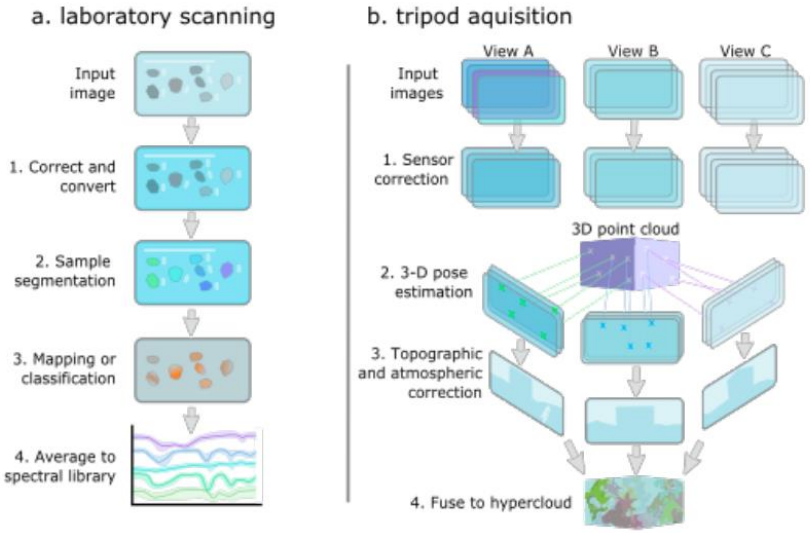

Data Analysis

1. False colour visualisation
2. Diagnostic feature mapping
  I.Estimate of mineral presence/absence
  II.Calculate clays crystallinity
3. Abundance mapping
  I. Extract pure-mineral spectra (end-members)
  II. Estimate mineral “abundance” (unmixing)
4. Facet detection and structural data extraction on photogrammetry model

TheiaX
Innovative Exploration

- The distribution of clay minerals often serve as proxy for mineralized zones. They also have an impact on separation processes and slope stability
- Great resolution which can refine the drill holes based (geometallurgical, resource, geotechnical) models.
- It can be implemented as real time tool in the workflow not just as an archiving tool.
- Possibility to move to drone to scan also pit-floor in order to better match the mining and processing workflow.

Tripod- and UAV-based Hypercloud Spectral Mapping of Pit Walls and Outcrops

Perspectives on pit mapping & refining resource model

- Possibility to integrate in resource estimate workflow pit mapping and pit scanning data to improve/refine the model
- The spectral data not necessarily has a direct implications in the distribution of ore minerals, but could help to improve alteration, structural and weathering constrains/models.
- Possibility to include in workflow also a higher resolution photogrammetry model and facet detection in order to obtain measures on vein and fault density and orientation. Quickly detects major faults and fractured zones.

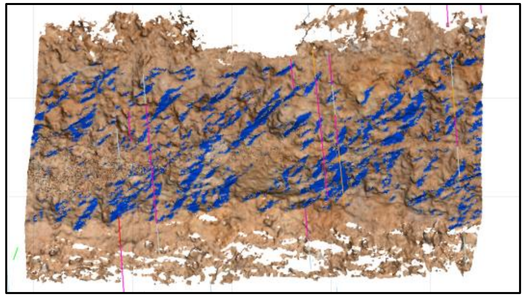

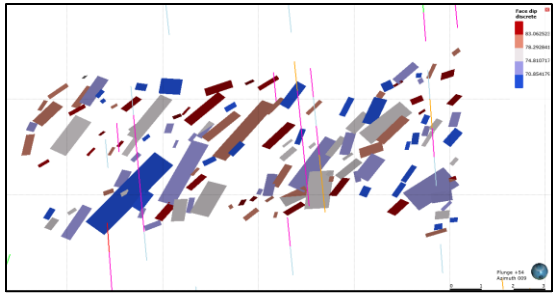

Pit wall with mapping and Au distribution

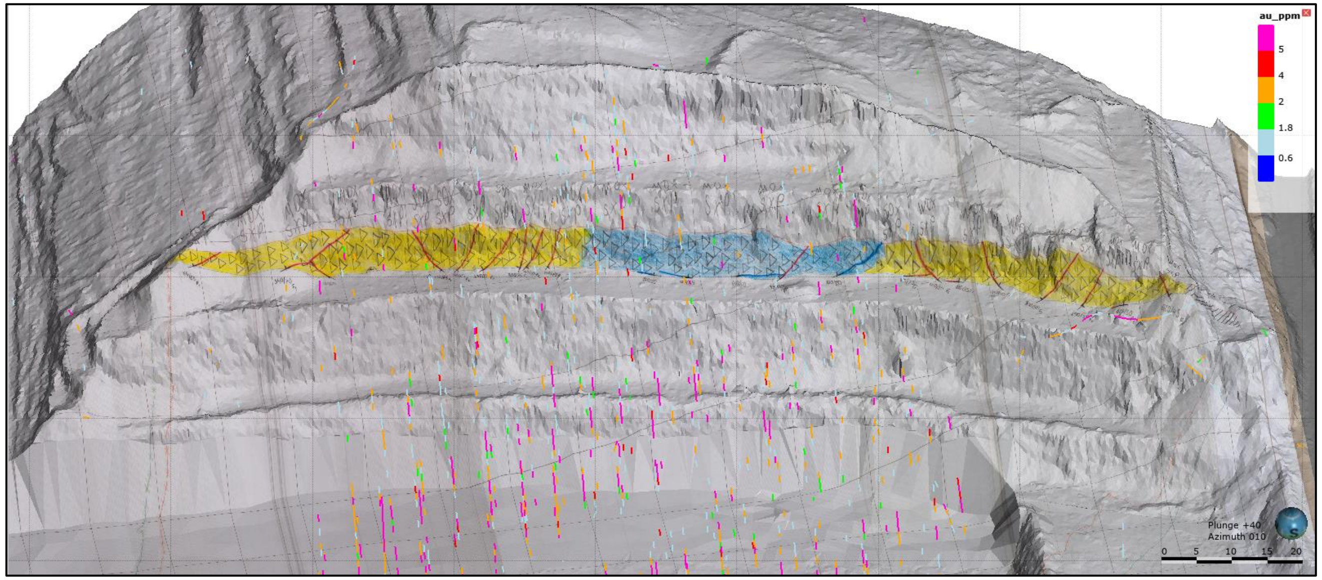

Pit wall enhanced color composite

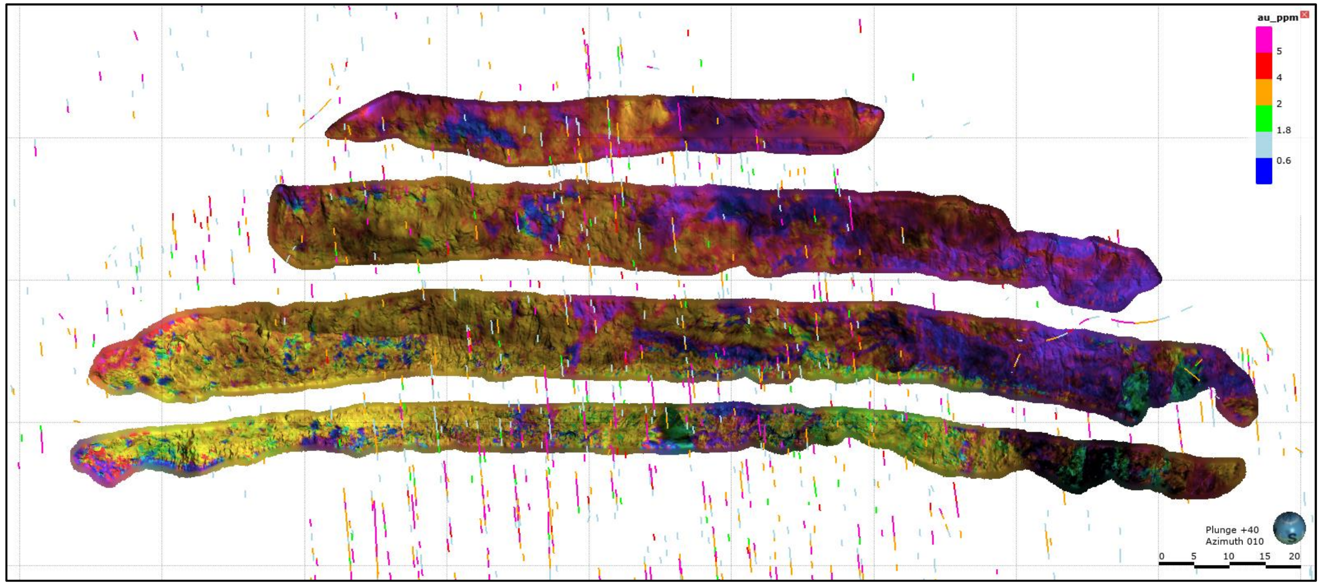

Tripod- and UAV-based Hypercloud Spectral Mapping of Pit Walls and Outcrops

Geometallurgical and geotechnical perspectives

- Detection of clay zones can be used real time for geotechnical planning, mining and processing.
- Kaolinite crystallinity and swelling clay abundance might became a key factor for metallurgical properties of many ore deposits, therefore hypercloud mapping/pit scanning could help to define/refine thresholds, map specific problematic areas and provide real time monitoring.

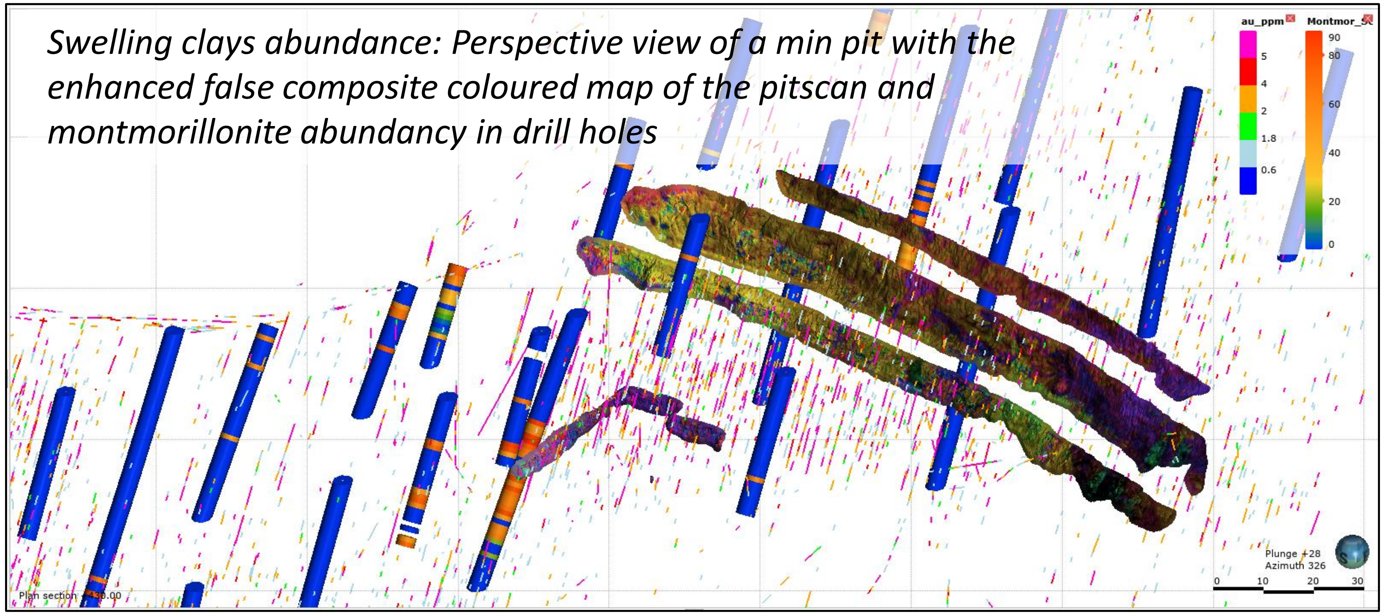
Swelling clays abundance: Perspective view of a min pit with the enhanced false composite coloured map of the pitscan and montmorillonite abundancy in drill holes

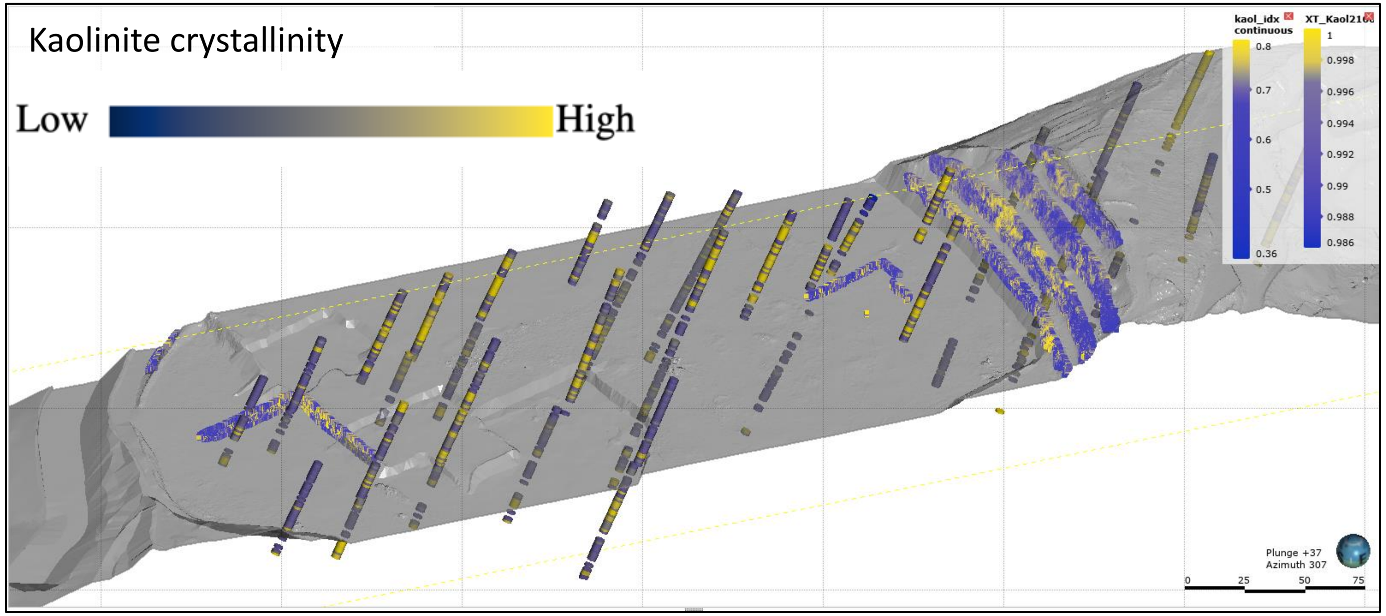
Kaolinite crystallinity

Satellite-based remote sensing in mineral exploration

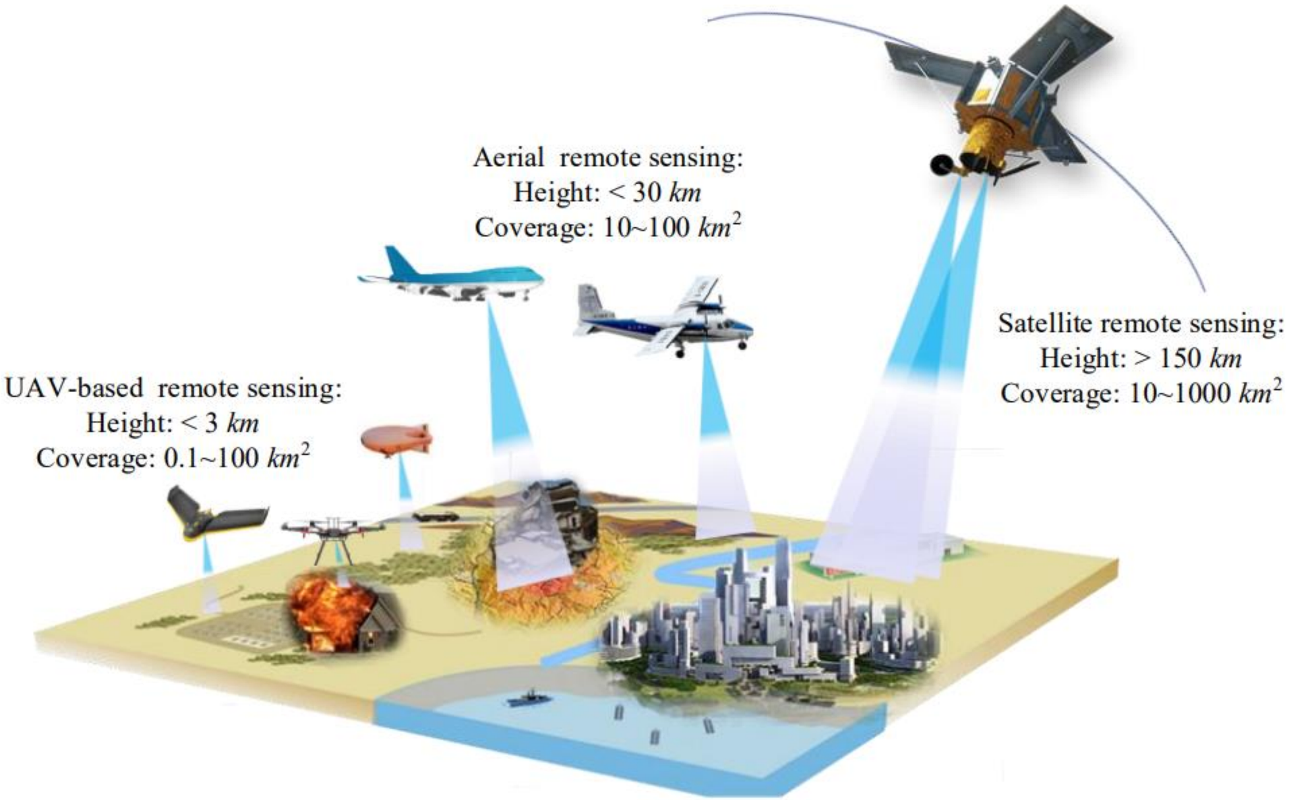

Satellite-based remote sensing in mineral exploration

Landsat-8, Sentinel-2, ASTER and WorldView-3 Spectral Imagery for Exploration

- Remote sensing has provided tools for geological exploration for almost four decades. Nowadays, many satellite remote sensing datasets are accessible freely and can be extensively used for mineral exploration projects.
- Multi-sensor satellite imagery can provide multiple sources of spectral data for mapping and discriminating hydrothermal alteration minerals to generate remote sensing-based prospectivity maps for metallogenic provinces.
- Works well specially on less-vegetated terrains.

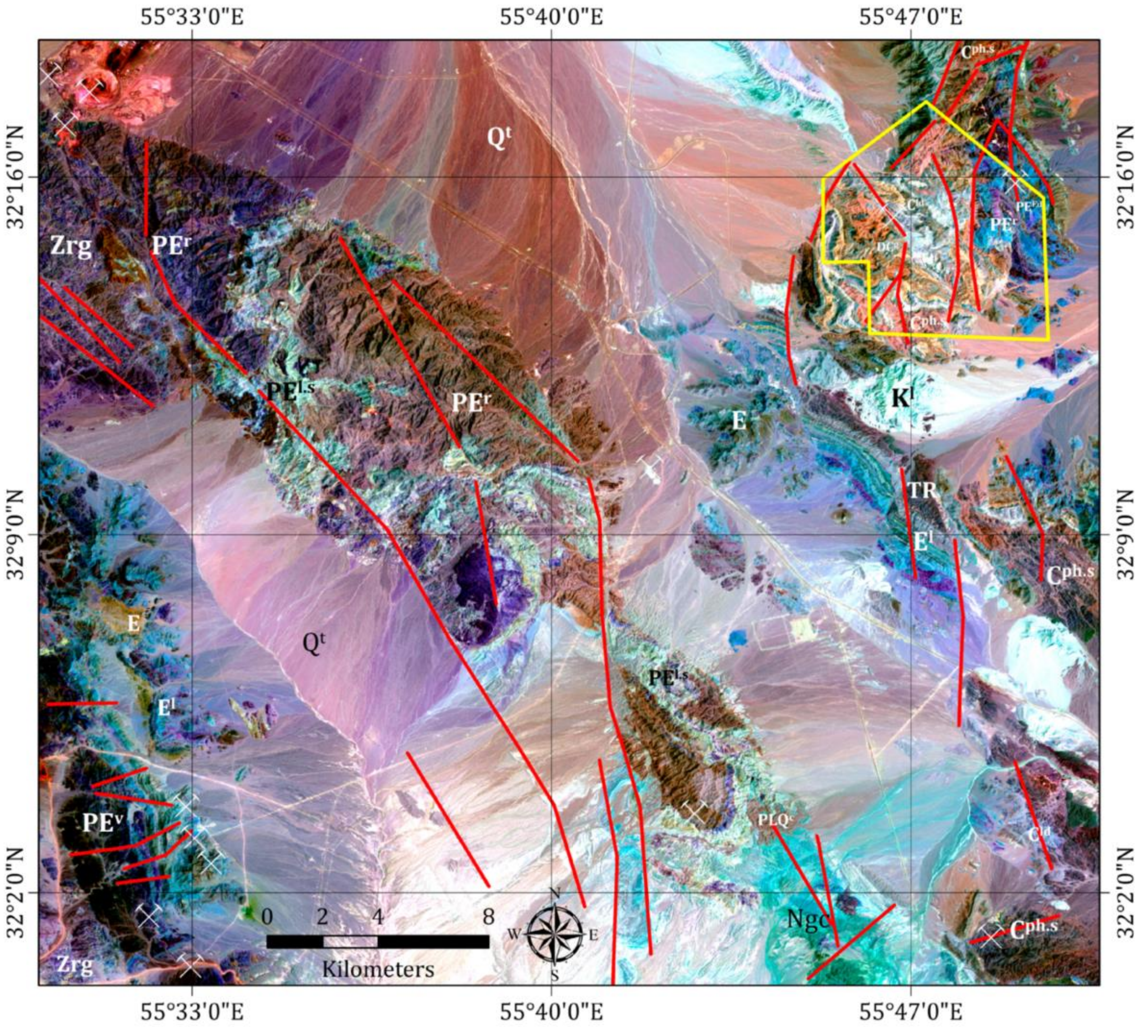

Regional view of lithological units and alteration zones in the studied region in Iran using RGB false color composite of bands 2, 8 and 12 for Sentinel-2. (Exploration of Carbonate-Hosted Pb-Zn Deposits in the Central Iranian Terrane, Sekandari et al. 2020).

Satellite-based remote sensing in mineral exploration

Technical performance and attributes of the Landsat-8, Sentinel-2, ASTER, and WV-3 sensors

- Landsat-8 imagery contains nine bands (0.433 to 2.290 µm; 30 m spatial resolution) in the VNIR and SWIR regions. The VNIR spectral bands are particularly sensitive for mapping iron oxides/hydroxides, while SWIR spectral bands are responsive for detecting hydroxyl-bearing minerals and carbonates. These spectral bands have been broadly used for mapping hydrothermal alteration zones associated with hydrothermal ore mineralizations.
- Sentinel-2 has thirteen spectral bands in the VNIR and the SWIR regions (0.433 to 2.280 µm; spatial resolutions from 10 to 60 m) which are useful to identify iron oxides/hydroxides and hydroxyl-bearing minerals.
- Six spectral bands in the SWIR range (1.600 to 2.430 µm; 30 m spatial resolution) allow the ASTER sensor to map clay and carbonate minerals. Detailed detection and discrimination of hydroxyl-bearing minerals and carbonates using ASTER SWIR bands is documented. Moreover, ASTER VNIR bands (0.52 to 0.86 µm; 15 m spatial resolution) can map iron oxides/hydroxides.
- The VNIR spectral bands of WV-2 and WV-3 (0.400 to 1.040 µm; 1.24 m spatial resolution) ca be used to discriminate Fe2+ and Fe3+ mineral groups. Al-OH, Mg-Fe-OH, CO3, and Si-OH alteration minerals were mapped in detail using SWIR bands of WV-3 (1.195 to 2.365 µm; 3.70 m spatial resolution).

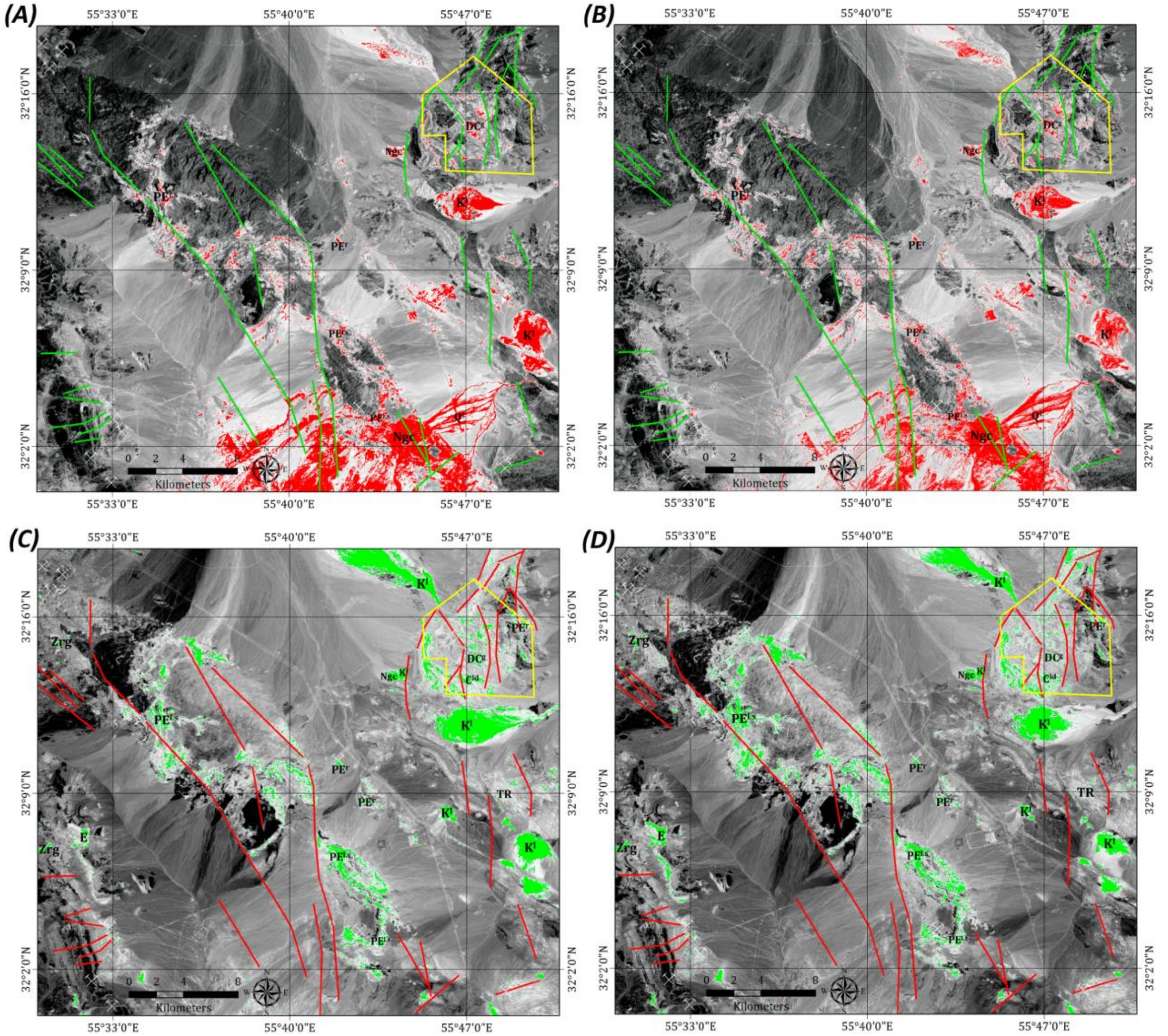

VNIR band ratio image-maps showing spatial distribution of iron oxide/hydroxides and clay and carbonate minerals at a studied region of Iran with Aster data (Exploration of Carbonate-Hosted Pb-Zn Deposits in the Central Iranian Terrane, Sekandari et al. 2020).

6. Distal ^{13}C/^{12}C and ^{18}O/$_{16}$O isotopes footprints in carbonate-hosted ore deposits

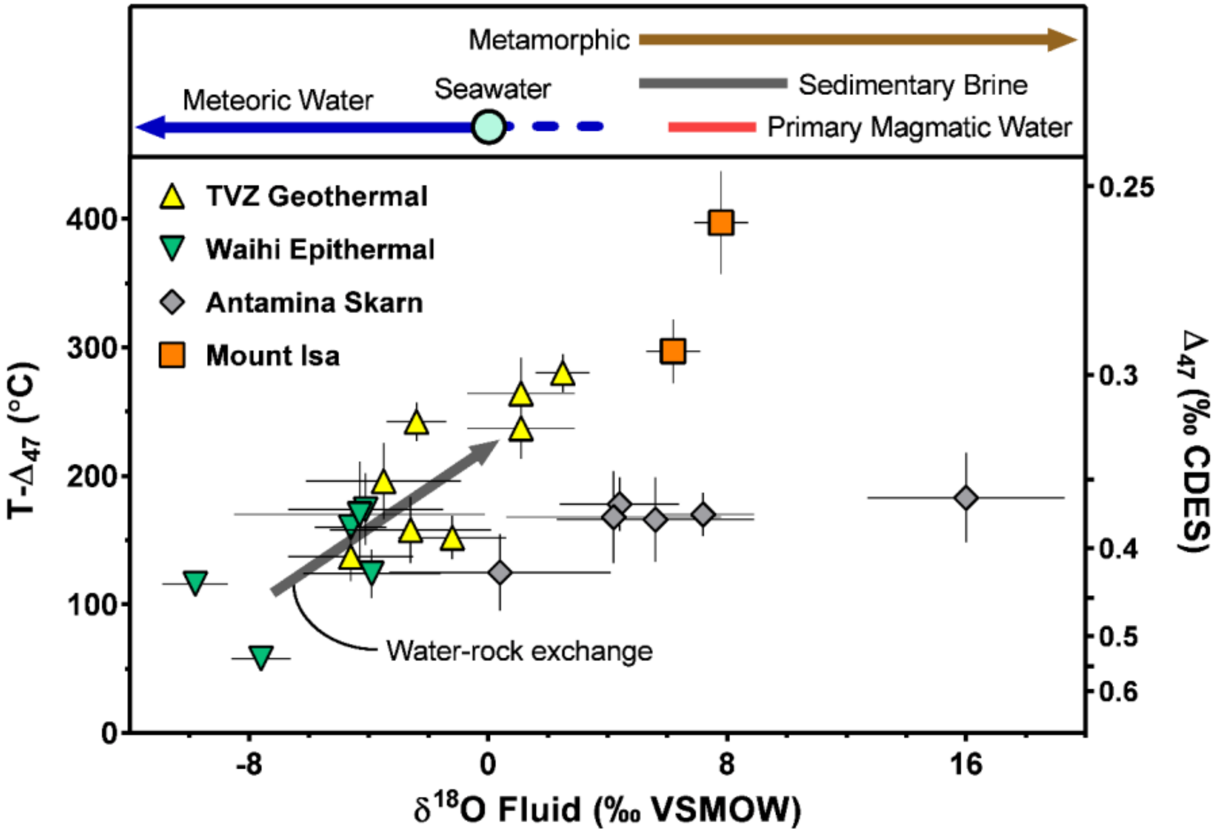

Distal ^{13}C/^{12}C and ^{18}O/$_{16}$O isotopes footprints in carbonate-hosted ore deposits

Mapping distal/broader alteration halos

- The trace-element hydrothermal alteration footprints of carbonate-hosted ore deposits are typically small and poorly developed, but the stable isotopes of carbon and oxygen in the carbonate rocks and veins indicate that fluid-rock interactions form much broader haloes that can be used in exploration vectoring.
- MDRU (University of British Columbia) have developed a mineral isotope analyser that allows for easier, faster and less expensive analyses of carbon and oxygen isotopes ratios (Barker et al., 2011).

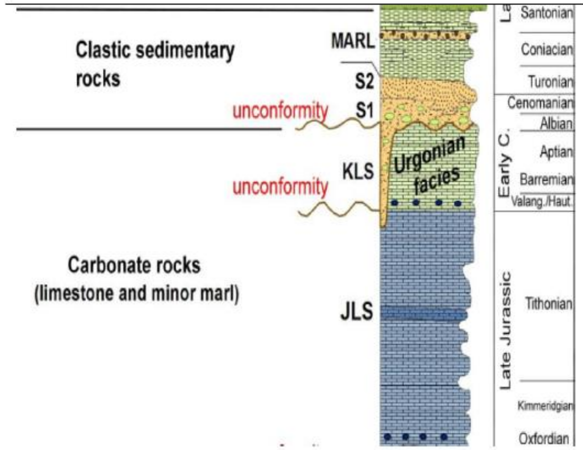

δ^{18}O (‰)	Samples from
22.4-25.1	Non-mineralized cover of the Bigar Hill
25.1-28.5	Korkan West
23.5-28.9	Non-mineralized footwall of the Bigar Hill
24.3-29.9	Tisnica Gorge, Korkan West

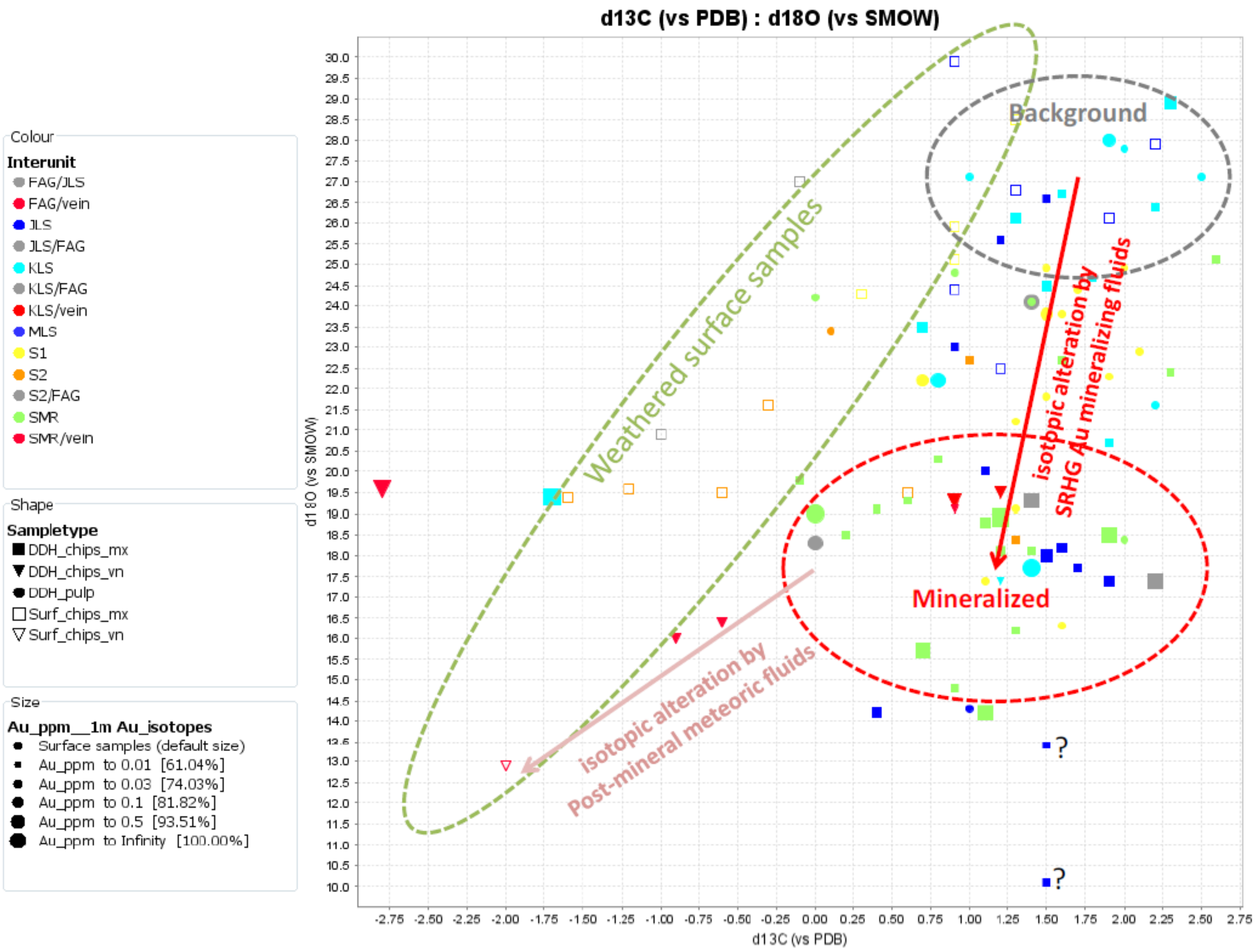

Oxygen and carbon isotopes ratios of samples analyzed from Timok, Eastern Serbia. The size of the symbols represents Au assay from the corresponding 1 meter drill assay interval where samples were collected for this study. Strongly mineralized intervals were not sampled for oxygen and carbon isotopes, as they do not contain carbonate minerals due to the extensive de-carbonatization associated by the mineralization.

Distal $^{13}C/^{12}C$ and $^{18}O/_{16}O$ isotopes footprints in carbonate-hosted ore deposits

Mapping distal/broader alteration halos

- δ18O data show systematic depletion within the non-mineralized marl toward the mineralized S2 unit from a (relative?) background value of 22.7‰;
- the oxygen isotopic footprint associated by a pervasive alteration exceed 40m (sample A69955) – well behind trace elements footprint;
- the δ18O isotope ratios for the pulp samples are systematically higher than for the corresponding core samples and do not follow well the trends set by the drill core samples.

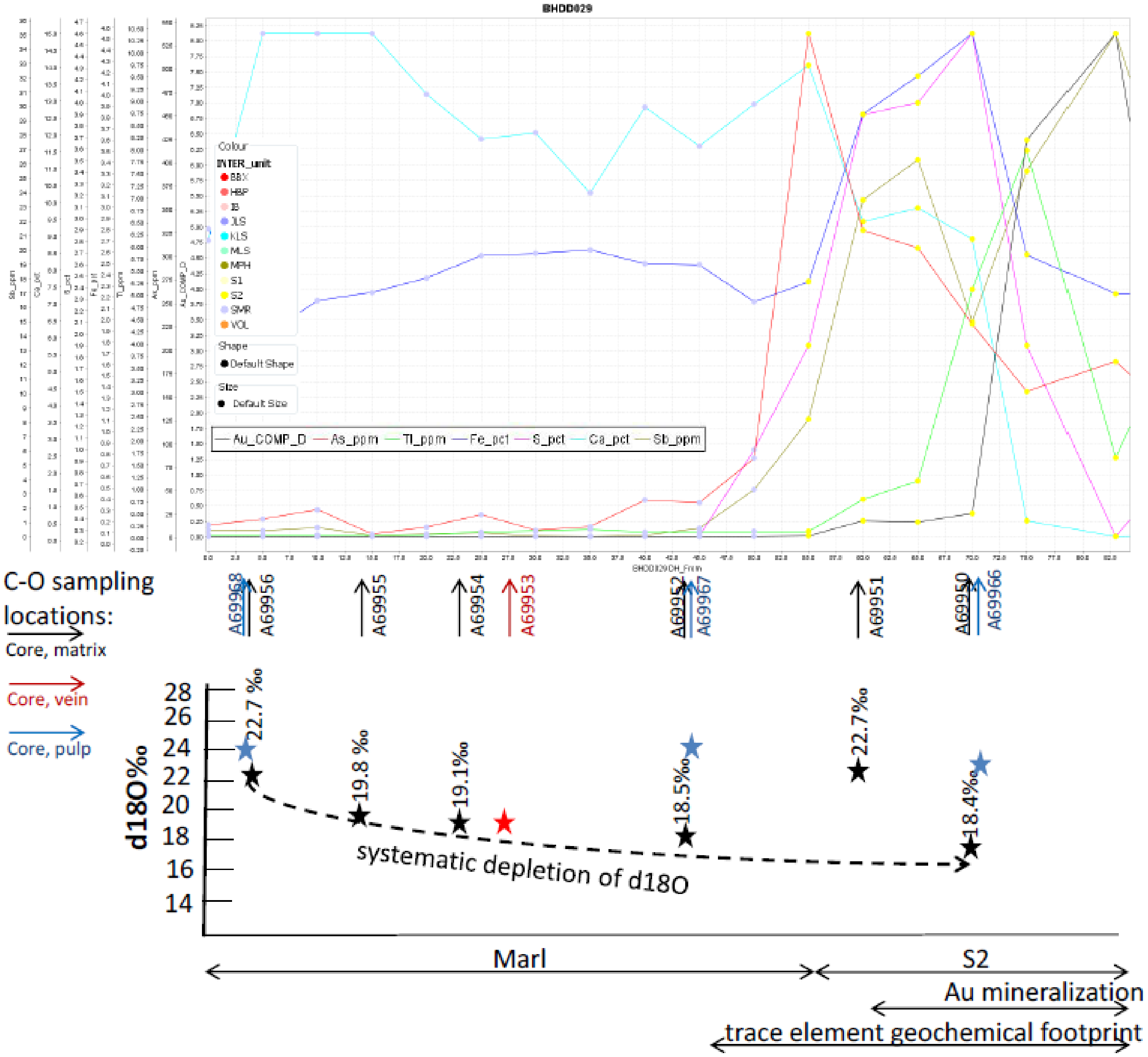

Distal $^{13}C/^{12}C$ and $^{18}O/_{16}O$ isotopes footprints in carbonate-hosted ore deposits

Mapping distal/broader alteration halos

- δ18O data show systematic depletion within the non-mineralized marl unit toward the mineralized zone from a (relative?) background value of 25.1‰;
- The oxygen isotopic footprint associated by a pervasive alteration exceed 50m (sample A69933);

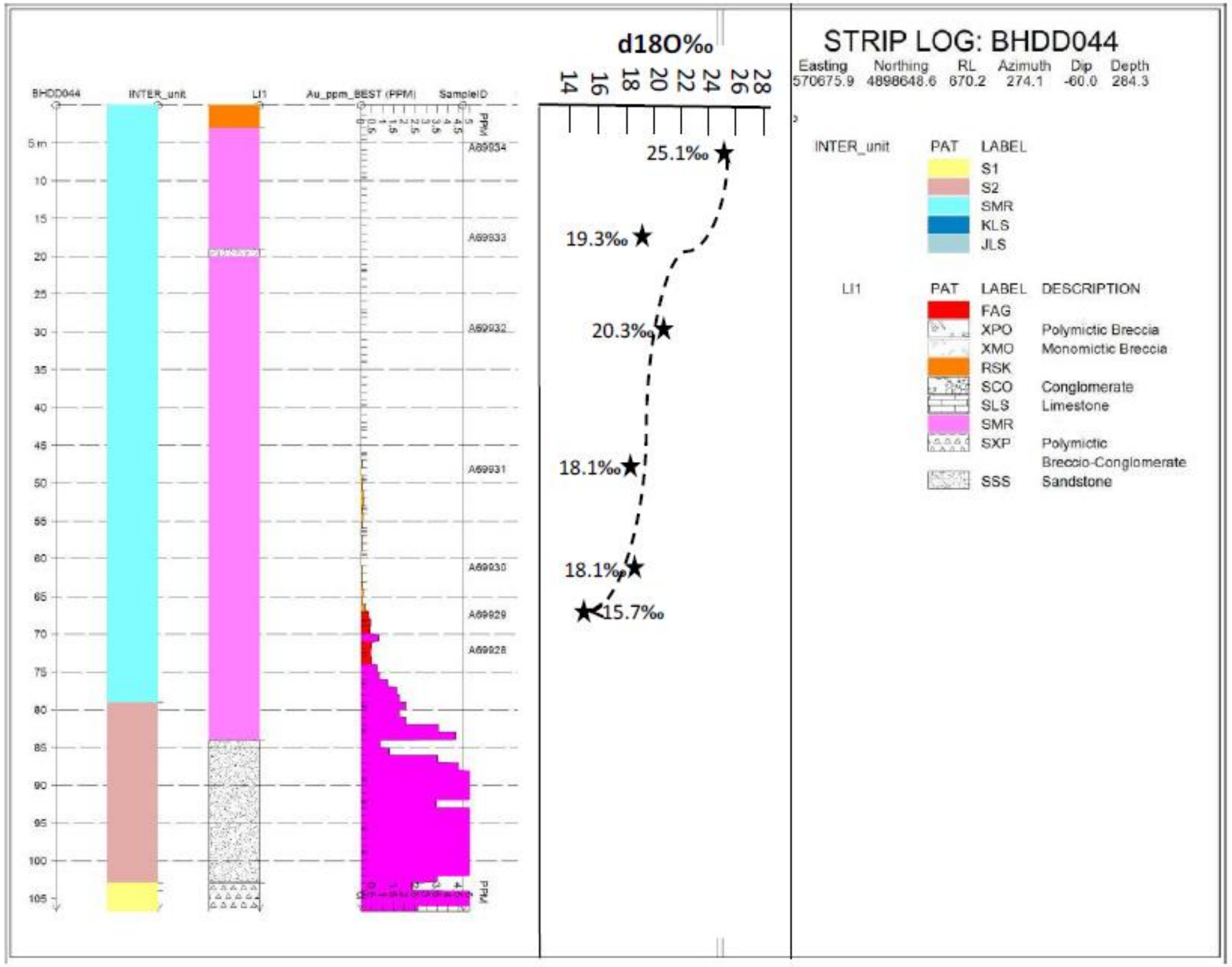

Long-term and creative professional collaboration environment and teamwork with Dundee Precious Metals and agreement to share exploration geochemical information for academic purposes is greatly appreciated.

Thank you for your attention!

DIM ESEE 2: IMPLEMENTING INNOVATIONS

Innovation in Exploration

Dubrovnik, Croatia / hybrid mode -
October 20th – 22nd, 2021